Geochemistry and origin of the Neoproterozoic Natkusiak Flood Basalts and related Franklin Sills, Victoria Island, Arctic Canada

Charles Beard [a,1], James S. Scoates[a], Dominique Weis[a], Jean Bédard[b] & Trent Dell'Oro[a]

[a]Pacific Centre for Isotopic and Geochemical Research, Department of Earth, Ocean and Atmospheric Sciences, University of British Columbia, 2020-2207 Main Mall, Vancouver, BC, V6T 1Z4, Canada

[b]Geological Survey of Canada, 490 de la Couronne, Québec City, QC, G1K 9A9, Canada

[1]Corresponding author, present address: Earth and Planetary Sciences, McGill University, 3450 University Street, Montreal, QC, H3A 0E8, Canada

Telephone +1 438 829 6677, email: charles.beard@mail.mcgill.ca

ABSTRACT

The Natkusiak continental flood basalts and Franklin sills of Victoria Island preserve an exceptional record of the ca. 716–723 Ma Franklin large igneous province and are synchronous with major climatic variations and breakup of the supercontinent Rodinia. The Natkusiak Formation basalts record an early phase of discontinuous rubbly flows (<100 m, low-Ti Type 1 magmas) overlain by a thicker series of extensive tholeiitic sheet flows (~1100 m, high-Ti Type 2 magmas). Coeval intrusions hosted by underlying Shaler Supergroup sedimentary rocks are differentiated low-Ti Type 1 Franklin sills and doleritic high-Ti Type 2 sills, both of which show correlations in isotope plots with the northernmost basalts on Victoria Island. Whole-rock Pb-Sr-Nd-Hf isotopic compositions from 66 samples indicate that the earliest magmas (Type 1) had similar primary melt compositions (Fo_{90} olivine) to oceanic island basalts and incorporated up to 10% granitoid basement (initial ε_{Nd} = –0.8 to –7, Nb/La = 0.42 to 0.67), a relatively weak continental signature compared to many other continental flood basalt provinces. Type 2 doleritic sills and the northern sheet flow basalts incorporated up to 5% granitoid (initial ε_{Nd} = +0.9 to +5.5), consistent with a waning continental influence during maturation of the magmatic system. Radiogenic isotope ratios are not correlated with indices of fractional crystallisation, which indicates that the continental material was either dispersed within the melt source, or that the magmas were heterogeneously contaminated prior to differentiation. In the southwestern part of Victoria Island, Type 1 basalts show negligible continental influence (Nb/La = 0.81 to 0.94) and have unusually high initial ε_{Nd} ratios (+4.4 to +11.8) that are decoupled from initial ε_{Hf} (+0.8 to +11.1). These radiogenic ε_{Nd} compositions persist throughout the southern volcanic stratigraphy and indicate involvement of a component with high time-integrated Sm/Nd that

lacked correspondingly high Lu/Hf. We suggest that the source region for the southwestern Natkusiak basalts and related sills included isotopically matured oceanic crust, which was recycled through the asthenospheric mantle into a laterally heterogeneous plume. The distinct trace element signatures of the southern and northern sources became attenuated with the onset of voluminous melting (corresponding to emplacement of the Type 2 doleritic sills and sheet flow basalts) and may reflect contributions from hydrous eclogitic material emplaced into the lithospheric mantle during the ca. 1.9 Ga Wopmay Orogeny. As both the northern and southern volcanic rocks exhibit contrasting isotopic signatures throughout the preserved stratigraphy, the magma plumbing system must have experienced limited lateral mixing and homogenisation, which allowed for the expression of distinct mantle source signatures in the high-level sills and basaltic lavas.

Key words: large igneous province; flood basalt; Pb-Sr-Nd-Hf isotopes; trace element, assimilation.

INTRODUCTION

Continental flood basalts form transient large igneous provinces that, together with oceanic plateaus and bolide impacts, represent the largest magmatic events preserved on our planet. Some 163 continental flood basalt (CFB) events have been identified in the geological record, ranging in size from 0.1 Mkm^2 to ~ 1 Mkm^2 (Ernst, 2014). As many CFB have been linked to the opening of new ocean basins, age correlations and alignments of associated dyke swarms are useful for palaeocontinental reconstructions (Ernst & Buchan, 2001; Bleeker & Ernst, 2006). The vast outpourings of noxious gases associated with some CFB are thought to have perturbed the global climate and triggered mass extinctions of terrestrial and marine life (Ganino & Arndt,

2009; Black *et al.*, 2014).

A unifying feature of large igneous provinces is their origin from unusually productive mantle sources, with most igneous material (>90 vol%) being emplaced in short pulses of 0.5–1 million years (Hooper *et al.*, 2002; Courtillot & Renne, 2003; Storey *et al.*, 2007). Such high melt fluxes require elevated mantle temperatures, which are commonly attributed to thermochemical mantle plumes (White & McKenzie, 1989; Campbell & Griffiths, 1990; Campbell, 2005). Evidence for uplift and lithospheric extension prior to the onset of volcanism is a common feature of CFBs, including the Franklin event of northern Canada, and is consistent with the plume model (Richards *et al.*, 1991; Rainbird, 1993; He *et al.*, 2003). Dense source materials, such as old oceanic crust, could dampen plume-related uplift, whilst still producing voluminous outpourings of basaltic melt (Sobolev *et al.*, 2009, 2011). The high melt fluxes in CFB provinces may at least partially result from unusually fertile sources containing abundant basaltic veins or stranded basaltic slabs (Turner & Hawkesworth, 1995; Garfunkel, 2008; Luttinen *et al.*, 2015). Xenolith studies reveal a wide variety of subcontinental lithospheric mantle rock types, which are variably metasomatised, hydrated, carbonated, or fertilised by small amounts of asthenospheric melt (Ionov *et al.*, 1993; Carlson & Irving, 1994; Zhang *et al.*, 2008). Melting of these different lithologies can yield a variety of melt compositions (Gudfinnsson & Presnall, 2005). For example, melting of hydrated peridotite yields basaltic melts (Mysen & Boettcher, 1975; Gaetani & Grove, 1998), whereas eclogite can, in some cases, generate more SiO_2-rich dacite or tonalite melts (Rapp & Watson, 1995; Yaxley, 2000). Partial melting of hydrated material can occur at relatively low solidus temperatures and will produce melts enriched in incompatible trace elements relative to the compositions of common flood basalts (McKenzie, 1989; Turner & Hawkesworth, 1995).

The major element composition of most CFB suggests they do not represent primary mantle melts, having differentiated on transit through the lithosphere (Cox, 1980; Francis *et al.*, 1981; Hooper & Hawkesworth, 1993). Most CFB show strong trace element and radiogenic isotope affinities with continental rock types (LILE-enrichment, negative Nb-Ta anomalies), suggesting significant inputs from metasomatised subcontinental lithospheric mantle or extensive assimilation of crustal rocks (DePaolo, 1981; Lightfoot & Hawkesworth, 1988; Lightfoot *et al.*, 1993; Jourdan *et al.*, 2007; Heinonen *et al.*, 2016). However, some CFB must have transited through the continental crust with minimal apparent chemical interaction. These relatively uncontaminated basalts may be used similarly to oceanic island basalts and oceanic plateaus as probes of mantle chemistry (Horan *et al.*, 1995; Kieffer *et al.*, 2004; Greene *et al.*, 2009; Weis *et al.*, 2011).

The Franklin Large Igneous Province (LIP) on Victoria Island offers an unprecedented opportunity to link a well-exposed magmatic plumbing system to a coeval volcanic succession in a large Neoproterozoic continental flood basalt province. The majority of well-studied LIPs are of Mesozoic and Cenozoic age, as older records have mostly been destroyed or degraded (Ernst & Bleeker, 2010). Because flood basalts are the products of fissure eruptions, the study of the Franklin sills as potential feeders for the coeval Natkusiak basalts is critical for determining the eruptive source area(s), the lengths of lava flows and the evolution of the magmatic architecture of this CFB province (Renne *et al.*, 1996; Vanderkluysen *et al.*, 2011). Additional factors, such as the intrusive/extrusive ratio and the type and degree of sedimentary rock assimilation may have influenced the environmental impact of Franklin magmatism (Ganino & Arndt, 2009; Sobolev *et al.*, 2011; Black *et al.*, 2014). CFB can trigger glaciation as a result of emissions of SO_2 or through CO_2 drawdown during basalt weathering (Cox *et al.*, 2016) or cause warming as

a result of CO_2 emission (Bond & Wignall, 2014). Quantifying the emissions associated with high-level crustal recycling in the Franklin LIP is of particular importance as its emplacement directly precedes the Sturtian global-scale glaciation (Hoffman *et al.*, 1998; MacDonald *et al.*, 2010).

In this study, we present whole-rock major element oxide, trace element, and Pb–Sr–Nd–Hf isotopic compositions for 66 samples of the Natkusiak basalts and Franklin sills, and from representative sedimentary host rocks of the Shaler Supergroup. We characterise the basaltic system in terms of its evolution and geochemical end-members, document systematic geographic and stratigraphic geochemical trends, investigate relative contributions from sedimentary host rocks and basement granitoids, and track the evolution of the mantle source regions for Franklin magmas. The excellent preservation and exposure of the Franklin rocks allow for comparisons with well-studied Phanerozoic continental flood basalt provinces and can be used to investigate how the character of CFB has changed through geologic time.

GEOLOGICAL SETTING

The Neoproterozoic Franklin LIP spans >2500 km, extending from Siberia to Greenland (Heaman *et al.*, 1992; Pehrsson & Buchan, 1999; Shellnutt *et al.*, 2004; Denyszyn *et al.*, 2009; Bédard *et al.*, 2012; Ariskin *et al.*, 2013) (Fig. 1). On Victoria Island, the Franklin LIP is expressed as the Natkusiak flood basalts and an intrusive suite of sills hosted by the Shaler Supergroup, which is dominated by shallow water clastic rocks, carbonates and sulphate evaporites (Rainbird, 1993; Thomson *et al.*, 2015). Exposure and preservation are excellent due to the lack of metamorphism and penetrative deformation (Thorsteinsson & Tozer, 1962; Bédard

et al., 2012). The Archean basement of Victoria Island comprises Slave Province granitoids (2.6–2.4 Ga) and is exposed on the northeastern coast (Fig. 2, Kolebaba *et al.*, 2003). S-wave seismic tomography indicates that the northern edge of a deep cratonic mantle root tracks along the north shore of Prince Albert Sound, directly south of the Minto Inlier (Harris, 2014). Franklin intrusions yield U-Pb zircon and baddeleyite ages of 723 +4/-2 Ma and 718 ± 2 Ma (Heaman *et al.*, 1992), coeval with the breakup of the supercontinent Rodinia (Li *et al.*, 2008) and the Islay carbon isotope excursion, which directly precedes the Sturtian glaciation (Macdonald *et al.*, 2010; Cox *et al.*, 2016).

The Natkusiak basalts crop out as two lobate erosional remnants within the shallow Holman Island Syncline (Fig. 2). The volcano-stratigraphic architecture is similar in both lobes (Baragar, 1976; Jefferson *et al.*, 1985; Williamson *et al.*, 2016). A basal sequence of hyaloclastite and rubbly flows (the V_0 lavas, 30 to >100 m thick) is locally interstratified with the underlying fluvial sandstones of the Kuujjua Formation in the southern lobe (Fig. 3b). The northern volcanic lobe has an unconformable lower contact with the Kilian Formation, which underlies the Kuujjua Formation (Fig. 2). The discordant basal Natkusiak contact was interpreted by Rainbird (1993) to reflect thermal doming of the lithosphere due to arrival of a mantle plume. Above the basal basalts is a discontinuous layer of valley-filling volcaniclastic deposits (clastic units C_1 and C_2, < 100 m thick, Williamson *et al.*, 2016). Laterally continuous sheet flow basalts cap the Natkusiak sequence on Victoria Island, and have a maximum preserved thickness of 1100 m in the northern volcanic lobe (Jefferson *et al.*, 1985). Two differentiation cycles are preserved in the northern volcanic lobe sheet flow basalts, each approximately 500 m thick (lava units V_1, V_2, Dostal *et al.*, 1986). Units above the lower massive member of V_1 are not preserved in the southern volcanic lobe (Williamson *et al.*, 2016) (Fig. 4).

The sedimentary rocks underlying the Natkusiak basalts host gabbroic and doleritic Franklin sills, which are typically 20–60 m thick (Baragar, 1976; Jefferson, 1985; Bédard *et al.*, 2012). Many sills are laterally continuous for tens of km (Hayes *et al.*, 2015c) and form cliffs between recessive sedimentary units (Rainbird, 1993). The oldest Franklin sill population (Type 1) has chilled margins with 6.5–13 wt % MgO and many have olivine-rich lower sections that are interpreted as cumulates (Hayes *et al.*, 2015b; Bédard *et al.*, 2016). Most Type 1 sills occur below the Wynniatt Formation (≥1.5 km palaeodepth), and are especially prominent to the north of the Minto Inlet and near Glenelg Bay (Fig. 2). Type 2 sills are generally more evolved than Type 1 sills, with chilled margins containing 6–8.5 wt % MgO (Bédard *et al.*, 2016) (Fig. 5). They may be plagioclase + clinopyroxene + olivine porphyritic to glomerocrystic and they occur throughout the stratigraphy of the Shaler Supergroup. Many Franklin sills are composite intrusions (Hayes *et al.*, 2015b, 2015c), and local crosscutting relationships demonstrate that Type 2 sills are younger than Type 1 sills. Field observations, whole-rock compositional shifts, mineral chemical zonation, and Pb and S isotopic data suggest that magma entered the sills as discrete pulses (Egorova & Latypov, 2013; Hryciuk, 2013; Hayes *et al.*, 2015c, 2015b). Replenishing pulses of magma may have been generated by a fault-gating mechanism in the upper crustal plumbing system (Bédard *et al.*, 2012), or may reflect lower crustal or mantle processes.

Below, we provide (1) a formal trace element classification of Type 1 and Type 2 Franklin magmas, and (2) divide these magma types into northern and southern subgroups, which allows for genetic interpretation on the basis of chemistry, Pb-Sr-Nd-Hf isotope composition and geographic position. With constraints from the volcanic stratigraphy (Williamson *et al.*, 2016), the petrography of the sills (Hayes *et al.*, 2015a, 2015b, 2015c), and

spatial control through new geological mapping (e.g. Bédard *et al.*, 2015), the trace element and isotopic geochemistry provides insight into the evolution of the Franklin LIP with respect to source components and composition, the extent of country rock assimilation, and differentiation of the magmas on their path from the mantle to the surface.

SAMPLING AND ANALYTICAL TECHNIQUES

Sample selection

Samples were collected during mapping and reconnaissance work with the Geological Survey of Canada in the summers of 2008, 2010 and 2011. The complete geochemical database is reported in Bédard *et al.* (2016) and includes major element oxide and trace element concentrations for 231 basalts and 2492 intrusive samples.

The 40 basalts analysed for radiogenic isotope compositions are from four widely spaced stratigraphic sections that were chosen to test for spatial variations in basalt geochemistry across the Franklin LIP (Fig. 2). A preliminary section through the northeast part of the northern lobe was sampled in 2008 (north section) and is complemented by reanalysis of archival samples from Baragar (1976; his sections 1B, 2B, and 3B). In 2010 and 2011, additional sections were measured and sampled throughout the southern lobe of the Natkusiak basalts (south and central sections) and the southern tip of the northern lobe (east section) (Dell'Oro, 2012; Williamson *et al.*, 2016). A total of 19 samples of intrusive rocks were analysed for isotopic compositions to establish differences between Type 1 and Type 2 sills, and to test for geochemical correlations between sills and the coeval Natkusiak basalts. The internal parts of the sills were sampled to

minimise the possibility of local host-rock contamination signatures. To aid in constraining the degree of assimilation of host-rocks, representative sedimentary rocks (n = 7) from the Shaler Supergroup were also analysed for major element oxide, trace element, and radiogenic isotope compositions. These are complemented by 197 analyses for major and trace elements of sedimentary rocks from the Geological Survey of Canada database (Bédard *et al.*, 2016). Sample locations were constrained by global positioning system (GPS) and are given in the Supplementary Data electronic appendices (supplementary data are available for downloading at http://www.petrology.oxfordjournals.org).

Analytical techniques

Samples were cleaned, crushed, and milled at the Pacific Centre for Isotopic and Geochemical Research (PCIGR), University of British Columbia (n = 43, see the Supplementary Data electronic appendices), the Institut National de la Recherche Scientifique (INRS), Québec City (n = 19), and the School of Earth and Ocean Sciences, Cardiff University (n = 4). Rocks processed at PCIGR were cut with a diamond-embedded tile saw to remove weathered surfaces and veins, then sandpapered under running water (e.g. Wright *et al.*, 1993). A total of 400 g of each sample was percussion-crushed between parallel WC plates and mixed thoroughly prior to pulverisation in agate planetary mills. Samples prepared at the INRS and Cardiff University were fragmented with a steel jaw crusher and pulverized in agate planetary mills. The evaporite samples (HY74A1a, BH166A1) were broken with a hammer and 100 g aliquots were hand-milled in an agate mortar. The shale sample (HY69A1) was ground directly with an agate planetary mill, bypassing the percussion crush step.

Major element oxide analyses were performed at INRS (n = 54), Carleton University,

Ottawa, Canada (n = 8, Williamson *et al.*, 2016), and Cardiff University (n = 4, Hayes *et al.*, 2015). Analyses at the INRS were by ICP-OES, calibrated against USGS reference materials BCR-2 and BHVO-2; full details of detection limits and analytical precision are summarized by Leclerc *et al.* (2011). Analyses at Carleton University were by fused-disc XRF, calibrated against the BCR-2 reference material. At Cardiff University, samples were fused with a lithium metaborate flux (McDonald & Viljoen, 2006), then analysed by ICP-OES, calibrated with JB1-a and NIM-g reference materials.

Trace element concentrations were determined at PCIGR (n = 37), INRS (n = 25) and at Cardiff University (n = 4). At PCIGR, fully digested samples were diluted ~5000 times in HNO_3 and analysed on an Agilent 7700 Quadrupole ICP-MS and Thermo Finnigan Element2 HR-ICP-MS, both calibrated with the BCR-2 reference material (Carpentier *et al.*, 2013; Schudel *et al.*, 2015). Instrumental drift was monitored with the internal standards Be, Re, Se, and In for the Agilent 7700, and with In (10 ppb) for the Element2. Trace element analyses at the INRS were by ICP-MS, following a method similar to that of Varfalvy *et al.* (1997); full details of detection limits and analytical precision are summarized by Leclerc *et al.* (2011). At Cardiff University, trace element concentrations were measured on a Thermo Elemental X7 Series ICP-MS. Analytical procedures and quality control measures are described by Neill *et al.* (2013).

High-precision Pb-Sr-Nd-Hf isotopic ratios were determined for 40 Natkusiak basalt samples, 19 Franklin sill samples, and seven Shaler Supergroup sedimentary rocks. Aliquots of powdered basalt were carefully acid-leached to minimise post-eruptive alteration effects (Weis *et al.*, 2005; Hanano *et al.*, 2009; Nobre Silva *et al.*, 2009, 2010). Powders of the basaltic and doleritic rocks were dissolved using the hot plate method of Weis *et al.* (2006), whereas powders of olivine-rich samples from the bases of sills, gabbros, and sedimentary rocks were digested in

high-pressure vessels (Pretorius *et al.*, 2006; Weis *et al.*, 2006). Anionic exchange columns were used to separate and purify Pb, Sr, Nd and Hf (see Connelly *et al.*, 2006; Weis *et al.*, 2006; Nobre Silva *et al.*, 2009 for procedures). Lead, Nd and Hf isotopic compositions were measured using a multi-collector (MC)-ICP-MS (Nu Instruments Ltd., Nu021). Analysis of NBS 981 during the course of the study yielded an average $^{206}Pb/^{204}Pb = 16.9433 \pm 20$, $^{207}Pb/^{204}Pb = 15.4998 \pm 23$, $^{208}Pb/^{204}Pb = 36.7205 \pm 87$ (n = 57). Analysis of Rennes Nd (MC-ICP-MS) gave an average $^{143}Nd/^{144}Nd = 0.511962 \pm 23$ (n = 42), and for JMC 475 the average was $^{176}Hf/^{177}Hf = 0.282171 \pm 32$ (n = 45). Strontium isotopic compositions, and neodymium isotopes for a select number of basalt samples, were measured by thermal ionisation mass spectrometry (TIMS, Finnigan Triton) at PCIGR (noted in Table 2). Analysis of NBS 987 yielded $^{87}Sr/^{86}Sr = 0.710253 \pm 15$ (n = 23) and for La Jolla Nd (TIMS) the average was $^{143}Nd/^{144}Nd = 0.511854 \pm 11$ (n = 4). The USGS reference materials BCR-2 and G-2 were analysed with the samples and yielded results within 2σ of published values (Weis *et al.*, 2006, 2007, data are given in the Supplementary Data electronic appendices). During the course of the study, internal reproducibility was tested by analysing 2–4 replicates (i.e. solution re-analysed) and 3–5 complete procedural duplicates (Tables 1 and 2). All Pb, Sr, Nd and Hf isotopic compositions were normalized to the published respective standard values (Weis *et al.*, 2006) and then they were age-corrected for *in situ* decay since 723 Ma (Heaman *et al.*, 1992). Decay constants used for age corrections are provided in the Supplementary Data electronic appendices.

RESULTS

Petrographic overview

The Natkusiak basalts are mostly aphyric to sparsely phyric rocks that have been metamorphosed at prehnite-pumpellyite facies conditions (a table of petrographic characteristics for the basalts is provided in the Supplementary Data electronic appendices). Sparse phenocrysts and glomerocrysts of clinopyroxene, plagioclase, titanomagnetite and olivine occur in some basalts. Some glomerocrysts may represent doleritic debris derived from the plumbing system. Dominantly subaerial alteration is manifest by the partial replacement of plagioclase by clay minerals, olivine by iddingsite and clinopyroxene by chlorite. Minor fractures, veins and amygdules (<1–35 vol. %, mm-cm scale) are filled with secondary chlorite, calcite, prehnite, quartz, and near vent areas, with native copper (Jefferson *et al.*, 1985). A petrographic catalogue of the basalt samples and chlorite chemistry is reported by Dell'Oro (2012) and additional descriptions can be found in Williamson *et al.* (2016).

The Franklin sills range from olivine ± clinopyroxene, to olivine + clinopyroxene + plagioclase, to clinopyroxene + plagioclase + titanomagnetite-phyric rocks. Petrographic textures of the Type 1 sills are described in detail in Hayes *et al.* (2015b, 2015c). The 10 samples presented here are pairs of olivine cumulate and doleritic rocks from five sites (Fig. 2) and were chosen to test whether the olivine-enriched bases of layered sills are cogenetic with the overlying dolerites. Type 2 sills have intergranular to subophitic textures and are dominated by clinopyroxene and plagioclase. Olivine phenocrysts are rarely present (e.g. in the Southern Feeder Dyke, Hayes *et al.*, 2015a). Secondary minerals comprise ~3–25% of the Type 2 sills that were analysed. Plagioclase is partially replaced by white micas, and clinopyroxene by chlorite ± opaque minerals. Interstitial material includes Fe-Ti oxides, base metal sulphides, minor amphibole and mica, and granophyric patches (e.g. JB123A). Carbonate-rich amygdules occur

near the upper contacts of some sills (e.g. HY74B2).

Effects of Alteration

Since eruption and emplacement at ~723 Ma, the Franklin sills and Natkusiak basalts have undergone metamorphism up to prehnite-pumpellyite grade. Secondary hydrothermal alteration is pervasive throughout the basalts. The least altered samples were selected for chemical analysis. The analyses of fluid-mobile elements (Na, K, LILE, Pb) were treated with particular caution, as they show significant variations in concentration, poor inter-correlations between major and trace elements (Figs 5a, 6), and poor correlations with radiogenic isotope compositions. The basalts are markedly depleted in Rb, Cs, Ba and Pb relative to the sills (Fig. 7). In contrast, the relatively immobile high field strength elements define linear trends in binary element diagrams, indicating that their concentrations were not affected by alteration or low-grade metamorphism (Fig. 6).

Major and trace element geochemistry

Major element oxide compositions are plotted in Fig. 5 and are included in the Supplementary Data electronic appendices. Most Natkusiak volcanic rocks and Franklin sills have tholeiitic basalt compositions with 45–51 wt % SiO_2 and 6–11 wt % MgO. Some samples show enrichment in Na_2O and K_2O that is probably the result of secondary alteration processes (Fig. 5a). The thin, basal unit of the Natkusiak lavas (V_0, 30–100 m) comprises high-Mg, low-Ti basalts (5.8–10.3 wt % MgO, 1.0–1.2 wt % TiO_2) with major element oxide compositions similar to chilled margins and dolerites of Type 1 Franklin sills. The thicker overlying sheet flow units (V_1 & V_2 , 1100 m total preserved thickness) are high-Ti basalts (1.2-1.8 wt % TiO_2) with compositions similar to the Type 2 Franklin sills. These Type 2 rocks have lower MgO (6–8 wt

%), higher FeO(t) and higher SiO_2 than the basal basalts, and their major element compositional trends are consistent with the effects of extensive igneous differentiation within this volcanic suite (Figs 4, 5). Type 1 Franklin sills are internally layered and samples that extend to relatively high MgO (18–24 wt %) and relatively low Al_2O_3 (6–11 wt %) are olivine cumulates (Hayes *et al.*, 2015b). In both the basalts and sills, the compatible elements Ni and Cr are positively correlated with MgO, reflecting the combined effects of olivine + chromite ± clinopyroxene fractionation and accumulation (Duke, 1976; see Fig. 6 from Dostal *et al.*, 1986). The Natkusiak basalts show moderate variations in the concentrations of Ni (78–157 ppm) and Cr (75–576 ppm) when compared to chilled margins from the Franklin intrusions (19–410 ppm and 50–1000 ppm, respectively; data in Bédard *et al.*, 2016).

Incompatible trace element compositions are illustrated in binary, chondrite-normalised, and mantle-normalised diagrams (Figs 6–7) and are included in the Supplementary Data electronic appendices. Chondrite-normalised rare earth element (REE) patterns are flat to slightly concave downward in shape, with some samples displaying weak negative Eu anomalies (Eu/Eu* = 0.85–1.11) (Fig. 7b). All samples are light REE-enriched, with the basal basalts and Type 1 sills characterized by steeper REE slopes than the sheet flow basalts and Type 2 sills (basalts: La/Yb = 3.1–4.1 *vs.* 2.3–3.1; sills: La/Yb = 1.7–11.8 *vs.* 2.4–12.5). Lanthanum concentrations range from 15–61 times chondrite and ytterbium concentrations from 3–31 times chondrite. Total REE concentrations are systematically higher in Type 2 rocks than Type 1 rocks and are highest in the strongly differentiated facies of Type 2 sills (i.e. high FeO*/MgO). Significant variation exists in the highly mobile large ion lithophile elements (LILE) Pb, Sr, Rb and Ba, reflecting variable degrees of alteration (Fig. 7a). When comparing Type 1 extrusive and intrusive rocks, it is apparent that some of the basalts have lost a significant part of their LILE

budget during subaerial alteration (Fig. 6). The immobile high field strength elements (HFSE) Nb, Ta, and to a lesser extent Ti, Zr, and Hf, display troughs in mantle-normalised diagrams that are most pronounced in the basal basalts and Type 1 sills. These elements form linear trends in binary diagrams (Fig. 6c, e, f) that can be used to distinguish the basal basalts from the sheet flow basalts (Fig. 6c). The Franklin sills display wider variability in incompatible element concentrations than the volcanic rocks as a result of intra-sill differentiation. In summary, major and trace element data support a formal correlation between Type 1 Franklin sills and the basal Natkusiak basalts, and between the Type 2 sills and Natkusiak sheet flow basalts.

Radiogenic isotope geochemistry

High-precision Pb, Sr, Nd and Hf isotopic compositions were collected for 40 Natkusiak basalts, 19 Franklin sills and seven Shaler Supergroup sedimentary host-rocks (Figs 3 and 8–10; Table 2). The basalts and sills are characterized by a wide range of initial $^{87}Sr/^{86}Sr$ (0.70250–0.70791), ε_{Nd} (+11.8 to -6.1), ε_{Hf} (+11.1 to -4.3), and Pb isotopic compositions that define coherent arrays ($^{206}Pb/^{204}Pb$ = 16.147–18.978; $^{207}Pb/^{204}Pb$ = 15.383–15.686; $^{208}Pb/^{204}Pb$ = 36.19–39.14). Basalts with initial $^{87}Sr/^{86}Sr$ above 0.705 are interpreted to reflect extensive alteration (i.e. Rb mobility, Fig. 8). The stratigraphically lowest basal Natkusiak basalts exhibit the widest range of initial $^{87}Sr/^{86}Sr$ (0.7025–0.7066) and $^{207}Pb/^{204}Pb$ (15.52–15.69) and isotopic variation decreases up-section into the sheet flows (central section, Fig. 4).

The three southern Natkusiak basalt sections (central, eastern and western sections) form a separate isotopic group from the Franklin sills and northern section Natkusiak basalts, with systematically higher initial ε_{Nd} (+4.0 to +11.8 *vs.* -6.1 to +8.8) and slightly less radiogenic Pb isotope ratios (Figs 8–10). The southern basal basalts (sampled only in the central section) have a

range of initial ε_{Nd} that is distinct from that of basal basalts from the northern section and the Type 1 sills. Conversely, the range of initial ε_{Nd} observed in the southern sheet flow basalts partially overlaps with the range of initial ε_{Nd} in the Type 2 sills and northern section sheet flow basalts (Figs 9, 11). The basal basalts (north and south) and Type 1 sills typically have higher initial $^{207}Pb/^{204}Pb$, $^{87}Sr/^{86}Sr$, and lower initial ε_{Nd} and ε_{Hf} when compared to the sheet flow basalts and Type 2 sills. Three of the five pairs of olivine cumulate bases and overlying doleritic rocks from individual Type 1 sills record internal heterogeneity in radiogenic isotope compositions, which implies that they are composite intrusions (*cf.* Hayes *et al.*, 2015b, 2015c).

Geochemical groupings and the spatial distribution of Natkusiak basalts and Franklin sills

The geochemistry of the Natkusiak basalts and Franklin sills on Victoria Island records contributions from a variety of mantle and lithospheric sources. As such, we have divided them into several chemical types and subgroups that reflect their distinct petrogenetic histories (Table 3). Type 1 low-TiO_2 magmas are preserved as the basal Natkusiak basalts and Type-1 Franklin sills and the younger, more voluminous Type 2 high-TiO_2 magmas comprise the Natkusiak sheet flow basalts and Type-2 Franklin sills. Both of these magma types are divided into northern and southern subgroups based on variations in trace element and radiogenic isotope ratios. *Northern Type 1* (n = 11) comprises Type 1 sills and northern section basal basalts (Unit V_0), which have low initial ε_{Nd} (-6.1 to -0.8), ε_{Hf} (-4.3 to +4.6), Nb/La (0.42–0.67) and high initial $^{87}Sr/^{86}Sr$ (0.7051–0.7075), suggesting the influence of continental materials (see Discussion below). *Northern Type 2* magmas (n = 16) are preserved as Type 2 sills and northern section sheet flow basalts (Units V_1 and V_2) and have higher initial ε_{Nd} (+1 to +8.8) and ε_{Hf} (+4.7 to +15.8) than the Northern Type 1 rocks, suggesting a waning influence of continental source materials.

Southern Type 1 rocks are basal basalts from the central section (V_0; n = 13, sheet flow basalts are the only exposed unit at the eastern and western sections) that have unusually high initial ε_{Nd} values (+4.4 to +8.3) that are below the terrestrial array in Nd-Hf isotope space (Vervoort *et al.*, 1999). Their high Nb/La (0.81–0.94) suggests limited continental influence, which contrasts with the Northern Type 1 rocks. Southern Type 1 rocks also have systematically higher initial $^{207}Pb/^{204}Pb$ for a given $^{206}Pb/^{204}Pb$ when compared to other Franklin rocks (Fig. 10a). *Southern Type 2* rocks comprise sheet flow basalts from the western, central and eastern sections (V_1; n = 13). These basalts have systematically higher initial ε_{Nd} (+4 to +11.8), lower $^{87}Sr/^{86}Sr$ and less radiogenic Pb isotope ratios than Northern Type 2 rocks, however, they are indistinguishable in terms of major element, trace element and Hf isotope compositions (Figs 8–10). All previous chemical studies on the Natkusiak basalts pertain to Northern Types 1 and 2 as the southern basalt sections were not systematically sampled and analysed hitherto (e.g. Dostal *et al.*, 1986; Dupuy *et al.*, 1995).

The Southern Type 2 basalts have systematically higher initial ε_{Nd} toward the southwest of the Minto Inlier (Fig. 11), which suggests a regional-scale control on magma contamination or source composition. Unusually high initial ε_{Nd} compositions persist throughout the volcanic stratigraphy of the central, eastern and western sections of the Natkusiak basalts (Fig. 4), indicating that the source of this geochemical heterogeneity was long-lived and voluminous. Northern Type 1 and Northern Type 2 rocks show no systematic geographic variations in radiogenic isotope composition (Fig. 11), which suggests that (1) there are no regional-scale spatial controls on their source composition or contamination, or (2) that both Northern Type 1 and Northern Type 2 magmas were isotopically homogenised in well-mixed magma chambers.

In the following sections, we discuss the origin and isotopic variability of the Natkusiak basalts and Franklin sills and present mixing models to support our hypotheses.

DISCUSSION

The principal factors that produce isotopic variations in continental flood basalts are: (1) variations in mantle source composition and (2) contamination by continental crust. The mantle source for continental basalts may be modified by earlier melting events (Vervoort & Blichert-Toft, 1999; Salters & Stracke, 2004) or may incorporate recycled subducted material (Zindler & Hart, 1986; White, 2010; Willbold & Stracke, 2010; Weis *et al.*, 2011), including rocks of continental origin (Barling *et al.*, 1994; Frey *et al.*, 2002). Continental geochemical signatures may also be acquired through assimilation of wall-rocks in crustal magma chambers (Wood, 1980; DePaolo, 1981; Huppert & Sparks, 1985; Spera & Bohrson, 2001) or through melting of subcontinental lithospheric mantle components that have been modified by subduction-related fluids or low-degree asthenospheric melts (Arndt & Christensen, 1992; Carlson & Irving, 1994; Turner & Hawkesworth, 1995; Hawkesworth *et al.*, 1999; Zhang *et al.*, 2008). The architecture of the magmatic plumbing system determines the degree of mixing and homogenisation of the magmas, and hence the potential for preservation of distinct geochemical source or contamination signatures (Marsh, 2004; Hayes *et al.*, 2015b).

The Franklin LIP compared to other Large Igneous Provinces

The range of radiogenic isotope ratios in the Franklin sills and Natkusiak basalts is narrow relative to many other large continental flood basalt provinces, which indicates that continental

materials likely played a comparatively smaller role in the evolution of the Franklin magmas (Figs 8–10). For example, the Natkusiak Formation lacks felsic volcanic units (e.g. Ewart *et al.*, 1998), and contains no highly contaminated units analogous to the Nadezhdinsky Formation of the Siberian traps, a ~400 m sequence of basalts that is characterised by a very low initial ε_{Nd} of -8 (Lightfoot *et al.*, 1993). No Franklin rocks exhibit the extreme continental isotopic compositions that are manifest in the lowermost Bushe Formation of the Deccan traps (initial ε_{Nd} down to -15 and initial $^{87}Sr/^{86}Sr$ up to 0.716, Cox & Hawkesworth, 1985). The Franklin rocks have both positive and negative initial ε_{Nd} values, in contrast with negative-only ε_{Nd} reported from the Ferrar dolerites in Tasmania (initial ε_{Nd} = -5.1 to -5.4, Hergt *et al.*, 1989). As defined by the range of trace element compositions presented in the full Victoria Island geochemical database (Bédard *et al.*, 2016), the analysed Type 1 Franklin sills in this study are biased towards the less continentally influenced samples (i.e. they are clustered toward the uncontaminated end of the compositional spectrum). The isotopic dataset, however, does cover the complete range of compositions indicating a contribution from continental crust. Even the most contaminated rocks show relatively low levels of continental influence compared to published results for Phanerozoic continental flood basalt provinces in general.

Tectonic classification diagrams using trace-element ratios suggest that the Northern Type 1 sills and basalts were derived from an enriched mantle source and that they mixed with variable proportions of continental materials (Pearce, 2008) (Fig. 12a). The sub-parallel mixing trajectory defined by the younger Northern Type 2 rocks indicates that they originate from a similar source to Northern Type 1 rocks with smaller continental contributions. Although the Pearce (2008) diagrams suggest a source with similar composition to plume-influenced E-

MORB, the radiogenic isotope variations are compatible with a source composition more akin to that of oceanic island basalts (OIB). Southern Type 1 basalts define a trend parallel to, and elevated relative to, the MORB-OIB array (Fig. 12a). This relationship suggests that the compositional variation is source-derived and does not result from variable degrees of assimilation of continental crust. Southern Type 2 basalts have compositions similar to Northern Type 2 sills and basalts.

Chondrite-normalised REE patterns for both Northern and Southern Type 1 rocks are consistent with a relatively low degree of melting (5–15%) of a mixed source of spinel lherzolite, with minor contributions from deep-seated garnet lherzolite (>90 km, Fig. 7b, Griselin *et al.*, 1997; Greene *et al.*, 2009). The flatter REE profiles of Type 2 rocks are consistent with smaller contributions from deep-seated garnet lherzolite (i.e. shallowing of the melt source, or higher degrees of melting) (Fig. 7b). As the ratio of TiO_2/Yb increases between Type 1 and Type 2 magmatism, a feature consistent with deepening of the source region (Fig. 12b), we suggest that the flattening of the REE profiles reflects an increase in the degree of melting in the plume head. In the following sections, we explore possible origins for the continental geochemical signatures in the Franklin basalts and sills, and discuss the spatial geochemical variations and their implications for the architecture of the magma plumbing system.

Constraining the parental melt compositions for the Franklin LIP

Whole-rock compositions from the least contaminated Northern Type 1 and Northern Type 2 magmas were used to calculate their respective primary mantle melt compositions. Parental melt major and trace element compositions for Northern Type 1 and Northern Type 2 magmas were calculated by incrementally adding equilibrium olivine to the most isotopically depleted samples

(JB-327b-01 and JB-08-01, respectively) until the calculated melts reached Fe/Mg equilibrium with Fo_{90} mantle olivine (Turner & Langmuir, 2015; Heinonen *et al.*, 2016); with 25% olivine being added to Type 1 melts, and 43% olivine to Type 2 melts. These olivine fractions are within 2% of those calculated with the PRIMELT3 model (Herzberg & Asimow, 2015). Trace element contents of the primary mantle melts were then calculated by back-fractionation of olivine, using olivine/melt partition coefficients calculated following Bédard (2005). Fractionation of olivine does not have a significant effect on incompatible element ratios, however, the absolute concentrations of incompatible elements are higher in fractionated melts. Primary melt compositions are indicated with stars on Fig. 13 and calculation methods are provided in the Supplementary Data electronic appendices.

Constraining possible high-level crustal contaminants

The Shaler Supergroup hosts the Franklin sills and is dominated by carbonate and sulphate evaporite sedimentary rocks with minor shale and quartz arenite (Rainbird *et al.*, 1994; Thomson *et al.*, 2015; Bédard *et al.*, 2016, compositions in Supplementary Data electronic appendices). Constraining the degree of assimilation of these rocks is useful for determining the potential CO_2 and SO_2 emissions associated with Franklin magmatism, and aids in the interpretation of geochemical signals of deeper magmatic processes. The carbonate and evaporite rocks are relatively rich in Sr and Pb, and poor in Nd and Hf, whereas rare shale beds are strongly enriched in incompatible trace elements and have the potential to exert significant influence on magmatic ε_{Nd} and ε_{Hf}. Quartz arenites have negligible trace element contents and are not considered further.

Below the Shaler Supergroup rocks are Archean granitoids of the Slave Province, which

constitute the basement for Victoria Island (Fig. 2). The Slave Craton is cross-cut by a major north-trending boundary delineated by contrasting Pb and Nd isotope compositions (Huston *et al.*, 2014). Samples from volcanic-hosted massive sulphide (VHMS) and gold deposits to the west and southwest of the province plot above the Stacey & Kramers (1975) two-stage model for terrestrial lead isotope evolution in $^{207}Pb/^{204}Pb$ *vs.* $^{206}Pb/^{204}Pb$ space, which is consistent with derivation from ~4 Ga protocrustal material (Thorpe *et al.*, 1992, Fig. SD3 in the Supplementary Data electronic appendices). To the northeast, these VHMS and gold deposits have more juvenile lead, with lower $^{207}Pb/^{204}Pb$ relative to $^{206}Pb/^{204}Pb$. Offset by ~100 km to the east is a similar boundary defined by Nd isotope compositions, with granitoids to the west having negative initial ε_{Nd} and those to the east characterised by positive initial ε_{Nd} (Davis & Hegner, 1992). Both isotopic data sets support derivation of eastern Slave crust from more juvenile material, and western Slave crust from older continental material (Davis *et al.*, 1996). There are currently no Hf isotopic compositions available for Slave Province basement rocks, so whether their assimilation can decouple the Nd and Hf isotope systems cannot be formally evaluated (Bill Davis, pers. com. December 2016). As the Franklin rocks plot on the Stacey & Kramers (1975) terrestrial lead evolution line, we suggest that evolved basement rocks with high $^{207}Pb/^{204}Pb$, such as those found in the western portion Slave Province, were not involved in their petrogenesis (Thorpe *et al.*, 1992). Some Slave Province rocks from the east may have been incorporated, however, because the Franklin rocks plot between the mantle and orogene compositions of Zartman & Doe (1981) in Pb isotope space, continental contributions cannot have been large (Fig. 10). Mixing models used to constrain the relative contributions from high-level crustal sources to Franklin magmatism are presented below.

Modelling crustal contamination of Franklin magmas

We use a simple bulk assimilation model to constrain potential geochemical and isotopic mixing trajectories, compare them to the Natkusiak basalts and Franklin sills, and use them to calculate the relative contributions from sedimentary country rocks and cratonic basement. Due to the variety of potential contaminants present, this is a simplified model for hypothesis testing and is used to establish plausible first-order petrogenetic mechanisms. Trace element compositions were calculated as bulk mixtures, whereas radiogenic isotope compositions were modelled following DePaolo (1981, modified from his equation 15).

The covariation of incompatible element ratios Nb/La, Ce/Sm, Th/Yb and Eu/Eu* with initial ε_{Nd}, ε_{Hf}, $^{87}Sr/^{86}Sr$ and $^{206}Pb/^{204}Pb$ suggests that the magmas incorporated continental material (Figs 13, 14). Conversely, the lack of correlation between radiogenic isotope compositions and major element abundances implies that contamination was not linked with progressive fractional crystallisation. Mixing models were chosen to reproduce the spread of trace element and radiogenic isotope ratios in the complete Victoria Island geochemical database (Bédard *et al.*, 2016) and to identify plausible contaminants. As each individual Shaler Supergroup lithology displays a wide range of trace element compositions (Bédard *et al.*, 2016), only rough estimations of assimilation proportions are possible.

Influence of sedimentary rock assimilation on magma compositions

Diagrams of ε_{Nd} *vs.* ε_{Hf} and Pb isotopic ratios show mixing trajectories between the average Type 1 sill composition and Shaler Supergroup shale and dolostone (Fig. 10 and Nd-Hf isotope diagram in the Supplementary Data electronic appendices). Although the choice of starting point is arbitrary, the mixing calculations nonetheless quantify the amounts of assimilation needed to account for the observed isotopic variability.

The correlation between the model mixing trajectories and the outlier geochemical characteristics of some Type 1 sills suggests that these magmas could have assimilated modest quantities (<10%) of Shaler Supergroup rocks. Chemical signatures indicate ≤10% of a dolostone contaminant in the Fort Collinson Sill Complex (Hayes *et al.*, 2015c, Fig. 10), and <10% assimilation of shale in Dick's sill. None of the model mixing trajectories with Shaler Supergroup compositions reproduced the trace element trends seen in the complete Victoria Island database (Bédard *et al.*, 2016). This suggests that the systematic chemical and isotopic variations between the geochemical groups defined above were not produced by high-level intra-crustal assimilation, but must originate from deeper parts of the magma plumbing system or at the source.

Constraining contributions from Slave Province granitoids to Franklin magmatism

Trace element ratio and isotope diagrams show mixing trajectories between calculated primary mantle melts for Northern Type 1 and Northern Type 2 Franklin rocks and Slave Craton granitoids (Fig. 13) (Davis *et al.*, 1994; Yamashita *et al.*, 1999). The correlation between the mixing models and the compositional range of Type 1 sills suggests that primary (Fo_{90}) Type 1 melts assimilated up to 10% Slave Province granitoids before emplacement (Fig. 13). The best-fit contaminant is a 1:1 mixture of two granodiorites from the Stagg and Awry suites that crop out ~50 km west of Yellowknife (samples Y-36 and Y-32 from Yamashita *et al.*, 1999). The compositional range expressed by the Type 2 sills correlates with a model mixture of up to 5% of the same granitoid with their respective Fo_{90} primary melt. This indicates that the continental contaminants to Franklin magmas remained similar through time, but that the extent of contamination waned as the magmatic plumbing system matured (Fig. 13). The mixing models were tested with Pb isotope compositions, however, the mixing ratios are inconsistent with the

Hf and Nd isotope and incompatible element ratio results. We infer from this that the U-Th-Pb system of the granitoids has not remained closed since their formation and that their parent/daughter element ratios were modified, perhaps during regional greenschist grade metamorphism (e.g. Babinski *et al.*, 1999).

Source components for the Franklin sills and Natkusiak basalts

The Northern Type 1 rocks have continentally influenced trace element and radiogenic isotope signatures (Figs 8, 9, 12, 13). In contrast, the Southern Type 1 rocks show no discernible continental crustal signature and have unusually high initial ε_{Nd} for a given ε_{Hf} (Fig. 9). These geographic distinctions in geochemistry weaken with maturation of the magmatic plumbing system (Type 2 magmas), although they do not disappear (Fig. 15). Despite isotopic differences, the major element compositions (Fig. 5) and physical volcanology of the Southern Type 1 and Type 2 basalts are comparable with the Northern Type 1 and Type 2 basalts, suggesting a similar petrogenetic history.

The initial $^{143}Nd/^{144}Nd$ isotopic compositions of the *Southern* basalts extend up to +7 ε_{Nd} units from the terrestrial array (Fig. 9b, nine epsilon units below the terrestrial array, or $\Delta\varepsilon_{Hf}$ of –9, see Nowell *et al.*, 2004) and record incorporation of material with high time-integrated Sm/Nd for a given Lu/Hf. Such signatures are unusual, as nearly all terrestrial rocks plot within the narrow, positively correlated terrestrial array on an $\varepsilon_{Nd} - \varepsilon_{Hf}$ diagram (Vervoort *et al.*, 1999, 2000). Available Hf isotope compositions for continental flood basalts and oceanic plateaus typically occupy the terrestrial array, with a few plotting above it ($\Delta\varepsilon_{Hf}$ up to +8, Ingle *et al.*, 2003; Tejada *et al.*, 2004; Greene *et al.*, 2008; Malitch *et al.*, 2009; Li *et al.*, 2012; Malitch *et al.*,

2013). Persistence of the high-ε_{Nd} isotope signature throughout the entire volcanic stratigraphy in the south of Victoria Island suggests that the geochemical anomaly was widespread, voluminous, and survived the first melt generation event. Southern Type 1 basalts also have lower Zr/Nb (~11) than all other Franklin rocks (Fig. 6c), elements that are not readily decoupled by variations in the degree of partial melting, or by crystallisation of olivine, clino- or orthopyroxene (Pearce & Norry, 1979). Below, we explore potential mechanisms for formation of decoupled Nd–Hf isotope signatures, as recorded in the Southern Type 1 and Southern Type 2 basalts. These isotopic variations may have been introduced into the basaltic magmas during incorporation of continental material or subcontinental lithospheric mantle, or they may have originated at the source (e.g. slivers of recycled crustal material in a heterogeneous mantle plume).

Origin of decoupled Hf and Nd isotopic signature of basalts from the central, eastern and western sections on Victoria Island

Zircon can decouple the $^{143}Nd/^{144}Nd$ and $^{176}Hf/^{177}Hf$ isotope systems because it has low Lu/Hf and high Sm/Nd relative to equilibrium melts (Rubatto & Hermann, 2007). Based on differential rates of physical and chemical weathering, Chauvel *et al.* (2008) proposed that zircon-rich sedimentary reservoirs can form in the continental crust, reservoirs which would evolve Nd-Hf isotope compositions below the terrestrial array. The Southern Type 1 and Type 2 basalts could not have inherited their high initial ε_{Nd} signatures from such a reservoir, as the Southern Type 1 basalts display limited geochemical evidence for interaction with continental rocks (e.g. narrow ranges of high Nb/La and low Ce/Sm, Th/Yb; Fig. 13) and do not show correlation between ε_{Nd} and Zr concentration (not shown). Southern Type 1 rocks also have low Zr/Nb, a feature that is

incompatible with melting of zircon-rich rocks (Fig. 6c).

A second possibility is that the mantle source for the Southern Type 1 and 2 basalts was modified by an earlier episode of melt extraction, whereas the source of the Northern magmas was not. A widespread low-degree melting event would have subtly increased Sm/Nd and decreased Rb/Sr and U-Th/Pb in the mantle residues without significantly affecting their Lu/Hf ratio. As the major and trace element systematics of the Northern Type 2 and Southern Type 2 rocks are very similar, only a small degree of melt extraction would be permitted within this model, thus offsetting Sm/Nd, Rb/Sr and U-Th/Pb without significantly affecting the major element composition or mineralogy of the source region for Southern Types 1 and 2 basalts. As such, incubation timescales would have to be long (probably >1 Ga) to produce a 6-unit increase in initial ε_{Nd} relative to the undepleted mantle source. A candidate event is the 1.27 Ga Mackenzie LIP, the locus of which lies near the Muskox intrusion, south of Victoria Island (Fig. 1) (LeCheminant & Heaman, 1989; Mackie *et al.*, 2009). In this scenario, the mantle south of Victoria Island would have experienced a low-degree melt extraction event associated with the edge of the Mackenzie mantle plume (Campbell & Griffiths, 1990), whereas the source of the Northern Franklin magmas would have been more distal, and less affected by this event. Alternatively, differential source depletion may have been associated with emplacement of the smaller Indin (2.12 Ga) or Ghost (1.89 Ga) dyke swarms (Buchan *et al.*, 2010, 2016). Although we cannot completely dismiss scenarios of prior differential depletion as an explanation for the Nd isotope shift seen in Franklin magmas, this model does not account for the low levels of continental contamination and low Zr/Nb observed in the Southern Type 1 basalts (Figs 14 & 6c). It has been suggested that a metasomatised source containing veins of low-Mg amphibole could produce basalts with relatively lower Zr/Nb, as Nb is more compatible in these minerals

than Zr (Tiepolo *et al.*, 2001). Although not inconsistent with a low-degree melt extraction event, this would require a later, voluminous input of volatile elements into the southern source region.

A third possibility is that the source for the southern Natkusiak basalts contained isotopically matured oceanic lithosphere. This model hinges on the ability of garnet to decouple the Nd and Hf isotope systems through preferential incorporation of Lu relative to Hf and Sm relative to Nd (Hauri *et al.*, 1994). As such, garnet-rich rocks would develop Nd-Hf isotope compositions above the terrestrial array (Vervoort & Patchett, 1996; Vervoort *et al.*, 2000) and melts that fractionated garnet, or were extracted from a garnet-bearing mantle restite, would generate Nd-Hf isotope compositions below the terrestrial array. Some modern oceanic basalts have steep chondrite-normalised rare earth element patterns suggestive of melting in the garnet stability field, and higher mantle potential temperatures earlier in Earth history may have promoted deeper melting in the presence of garnet (Arndt, 1983; Xie *et al.*, 1993; Hirschmann & Stolper, 1996; Pearce, 2008). Ancient oceanic crust, sourced from deep, hot, mantle could therefore have developed Nd-Hf isotope compositions below the terrestrial array, provided that its Lu/Hf and Sm/Nd were not significantly modified during subduction.

To test this hypothesis, we modelled the Nd-Hf isotopic evolution of several mafic to ultramafic Archean and early Proterozoic rocks of suggested oceanic origin following calculations from Nowell *et al.* (2004) (Fig. 9b). A suitable Nd-Hf maturation trajectory was produced using 2.7 Ga Al-undepleted 'Munro-type' Archean komatiites from the Abitibi belt in Canada and from the Belingwe belt in Zimbabwe (Blichert-Toft & Arndt, 1999). Using these compositions, ε_{Nd}–ε_{Hf} isotopic compositions similar to the Southern Type 1 and Southern Type 2 rocks can be generated in as little as 1 Ga (Fig. 9b). Palaeoproterozoic Chukotat group

tholeiitic basalts from the Cape Smith belt, Canada (Vervoort & Blichert-Toft, 1999) also develop Nd-Hf isotope compositions below the terrestrial array, but do so more sluggishly than the Munro komatiites as they produce matured compositions similar to the Southern Type 1 and 2 basalts in 2.5 Ga. This suggests that, if storage time is limited (< 1 Ga), a pure tholeiitic source is unlikely, and that komatiitic material probably played at least a partial role. Shown for comparison in Figure 9b are some Al-depleted komatiites from the Barberton greenstone belt in South Africa (Blichert-Toft & Arndt, 1999) and a basaltic andesite from the Abitibi belt, Canada (Vervoort & Blichert-Toft, 1999). Their evolution trajectories appear to discount major involvement of these rock types in the source for the Southern Type 1 and Southern Type 2 rocks.

Tectonic context for the involvement of matured oceanic lithosphere in the source for Franklin magmas

During the Wopmay Orogeny (ca. 1.9–1.8 Ga), oceanic lithosphere was emplaced below the western margin of the Slave Province (Hoffman & Bowring, 1984; Smart *et al.*, 2014). This lithosphere is now preserved as eclogites, xenoliths of which have been recovered from the Jericho and Diavik kimberlite pipes on the Canadian mainland, south of Victoria Island (Schmidberger *et al.*, 2005, 2007). The Jericho eclogite xenoliths have a wide range of zircon U-Pb dates and zircon Hf depleted mantle model ages extending to 2.1–2.0 Ga and their petrography records a complex geological history, punctuated by metasomatism and melt extraction events (Schmidberger *et al.*, 2005; Smart *et al.*, 2009). Phlogopite and zircon contained within the Jericho eclogites have the potential to decouple Zr and Nb concentrations on melting (Pearce & Norry, 1979) (Fig. 6c), and hydrated material would produce melts enriched in incompatible elements (e.g. elevated Th, Fig. 12a) (McKenzie, 1989; Turner &

Hawkesworth, 1995). These geochemical signatures are both observed in the Southern Type 1 basalts. Additionally, fluids released during melting of hydrous minerals may have increased the buoyancy of Southern Type 1 magmas (Ochs & Lange, 1999), boosting ascent rates and minimising the interactions between Southern Type 1 magmas and continental crust (Figs 12a, 13).

If this body of ancient, eclogitised oceanic lithosphere extended northward below Victoria Island, it may have been present in the source region for the Southern Type 1 and Southern Type 2 Natkusiak basalts (Fig. 15). The age constraints on the eclogite xenoliths provide ample time for incubation of suitable Nd-Hf isotope compositions prior to the Franklin magmatic event (1.2 to 1.4 Ga), in accord with our isotope model discussed above (Fig. 9). The results of the modelling favour influence from matured oceanic lithosphere that was initially produced by high degrees of mantle melting. Therefore, the source region for the Southern Natkusiak basalts may have contained an underthrust or underplated oceanic plateau, possibly including komatiite (Storey *et al.*, 1991). The presence of dense, old oceanic crust in the melt source may have dampened the uplift effect of the arrival of a thermochemical mantle plume (Sobolev *et al.*, 2009, 2011). This is consistent with limited uplift in the south of Victoria Island, relative to the north, as recorded by the sequence of sedimentary rocks of the upper Shaler Supergroup (Rainbird, 1993).

Nd-Hf isotope compositions for eclogite xenoliths from the Diavik kimberlite suggest that Wopmay-derived material was not responsible for the distinctive Nd isotope composition of the southern Natkusiak basalts (Schmidberger *et al.*, 2007). However, the Diavik xenoliths have been influenced by metasomatic and melt extraction processes that may have affected their isotopic evolution. Involvement of underplated lithospheric material cannot be completely

discounted, because kimberlites from Somerset Island record lateral variations in lithospheric character, with Nd-Hf isotope compositions that fall slightly below the terrestrial array (Schmidberger *et al.*, 2002).

Persistence of distinct Nd isotope compositions during Type 2 magmatism and deep recycling of matured oceanic lithosphere

The Southern Type 2 basalts are more voluminous than the Southern Type 1 basalts and have major and trace element compositions indistinguishable from their northern counterparts (Figs 4–5). Despite homogenisation of trace element compositions, the high initial ε_{Nd} isotopic signature manifest in the Southern Type 1 basalts persists at a similar magnitude throughout the volcanism that produced the Type 2 basalts (~ +5 ε_{Nd} units from the terrestrial array, Fig. 9). As such, the source component is unlikely to have resided in the lithospheric mantle, because such material would be cold and refractory, hence unlikely to melt extensively (Arndt & Christensen, 1992; Arndt *et al.*, 1993). If somehow the lithospheric mantle did melt, it would likely be rapidly exhausted.

An alternative hypothesis is that distinctive isotopic flavours were present in the Franklin plume, much like those that are documented in the Loa and Kea trend basalts preserved in the Hawaiian islands today (Weis *et al.*, 2011). Plume heterogeneity might reflect variable contributions from matured oceanic lithosphere, which were recycled into the asthenospheric mantle long before the onset of Franklin magmatism. Unfortunately, no hard time constraints may be placed on this model, and it cannot account for variability in the trace element chemistry and evidence for differences in extents of assimilation between the Northern and Southern Type 1 rocks (Figs 6c & 13). Incubation timescales are likely to have been long (> 1 Ga), because the

major and trace element compositions of Northern Type 2 and Southern Type 2 rocks are indistinguishable. This implies that the northern and southern mantle sources had similar mineralogy and composition.

Implications for origin and evolution of the Franklin large igneous province

The isotopic dataset from the Natkusiak basalts and Franklin sills reveals that lateral compositional variations in the melt source region for CFB may persist for timescales of 100s of Ma to Ga. Lateral variations of initial ε_{Nd} in the Type 2 basalts indicate that subtle source heterogeneities can survive earlier melting events and confirm that voluminous melting affected a laterally heterogeneous source mantle (Campbell & Griffiths, 1990). These data also demonstrate that CFB magmas can erupt with incomplete lateral mixing and homogenisation on the 50–100 km scale (e.g. Arndt *et al.*, 1998) (Fig. 15). The decoupling of indices of fractionation from upper continental crustal geochemical signatures in Franklin magmas is compatible with an RTFA-type system, in which large volumes of magma with a small range of crystallisation-buffered compositions can be generated (Figs 4 & 5, i.e. periodically replenished and tapped whilst fractionating crystals and assimilating wall-rocks, O'Hara & Mathews, 1981; Cox & Hawkesworth, 1984; Wooden *et al.*, 1993). Systematic lateral changes in initial ε_{Nd} in the Southern Type 2 basalts suggest that mixing and homogenisation had a limited effect, and that source signatures were effectively transferred to the surface (Figs 11, 15). Conversely, the lack of systematic spatial variation in initial ε_{Nd} in the Northern Type 1 and Northern Type 2 magmas suggests they may have intruded laterally beneath eruptive regions for Southern Type 1 and Southern Type 2 basalts. Lateral changes in the geochemistry of the Franklin sills indicate that at least some intrusions propagated towards the southwest (cf. Hayes *et al.*, 2015b). None of

the sampled intrusions have suitable Nd-Hf isotope compositions to represent feeders for the southern Natkusiak basalts, however sills exposed in the west and south of the Minto Inlier were not analysed in this study (Fig. 2) and may preserve an isotopic boundary. Although the Coronation sills to the south of Victoria Island have high initial ε_{Nd} (Fig. 1) (Shellnutt *et al.*, 2004) their Hf isotope compositions have not been measured, so a genetic link with the Southern Natkusiak basalts cannot be confirmed (Fig. 9a).

The effects of Franklin magmatism on global climate remain poorly constrained, due largely to uncertainties in the volume of sedimentary rock that was assimilated by the Franklin magmas or affected by their thermal haloes (e.g. Nabelek *et al.*, 2012). Recent mapping efforts have constrained the distribution and proportion of Franklin sills within the Shaler Supergroup (Fig. 2) (e.g. Bédard *et al.*, 2015), however, quantifying the amount of assimilated sedimentary rock remains a challenge. Further work is needed to evaluate the effects of Franklin magmatism on the Neoproterozoic climate and the relationship with Sturtian glaciation (Macdonald *et al.*, 2010; Cox *et al.*, 2016).

CONCLUSIONS

The geochemistry of the Franklin sills and Natkusiak basalts of Victoria Island allows for comparison of the feeder system and volcanic products of a large Neoproterozoic continental flood basalt province. During initiation, lateral variations in source composition defined the character of magmatism. Low-TiO_2 basalts with a continental influence ascended through Type 1

Franklin sills, erupting as basal Natkusiak basalts in the north. Uncontaminated low-TiO_2 basal basalts were emplaced only in the south. As the degree of melting in the plume head increased, flood basalt volcanism reached its zenith during high-TiO_2 Type 2 magmatism. Emplacement of doleritic Type 2 sills remained limited to the northern source region, despite waning differences in source signatures between northern and southern magmas. The northern Natkusiak flood basalts geochemically match the Franklin sills, with Type 1 sills corresponding to the thin basal basalts and Type 2 sills linked to the overlying sheet flow basalts. Assimilation modelling shows that Type 1 Franklin sills can be reproduced by mixing of up to 10% Slave Province granodiorite basement rocks into their primary asthenospheric melts (Fo_{90} olivine), followed by small amounts of assimilation of a variety of Shaler Supergroup metasedimentary rocks (<<10%). Younger Type 2 sills have slightly more primitive primary melt compositions and a weaker continental influence that can be explained by incorporation up to 5% of the same granitoids. Toward the southwest of Victoria Island, the Natkusiak basalts record progressively higher initial ε_{Nd} values, which are decoupled from ε_{Hf} and displaced below the terrestrial array on an Nd-Hf isotope diagram. None of the Franklin sill samples exhibit this isotopic offset, however, the Coronation sills, located south of Victoria Island, may represent part of the southern feeder system. As the displacement below the Nd-Hf isotope terrestrial array is of a similar magnitude for the Southern Type 1 and Southern Type 2 basalts, their source regions appear to have shared similar, or at least linked, histories. The source regions for northern and southern magmas of the Franklin large igneous province were broadly similar, except for (1) a greater hydrous component in the southern source region, which was consumed during the initial phase of volcanism (low Zr/Nb, high Th), and (2) significantly higher time-integrated Sm/Nd (i.e. higher initial ε_{Nd}). The former might reflect contributions from altered Palaeoproterozoic oceanic crust,

emplaced below the Slave Province during the ca 1.9 Ga Wopmay Orogen, and demonstrates the influence of cratonic lithospheric mantle architecture on the geochemistry of the continental flood basalts and related high-level intrusions. The persistence of Nd-isotopic heterogeneities throughout all stages of development of the Franklin large igneous province resulted from lateral compositional variations within the mantle plume, and likely reflects contributions from isotopically matured Archaean or Palaeoproterozoic oceanic lithosphere that was recycled deep into the asthenosphere.

ACKNOWLEDGEMENTS

We thank the entire field crew of the Geomapping for Energy and Minerals (GEM) program for two unforgettable summers of mapping in the Canadian Arctic. Their efforts have been instrumental in constructing the Victoria Island geochemical database from which the samples presented here were selected. Special thanks are due to Rob Rainbird for his invaluable organizational work. Thanks to Ben Hayes, Matt Hryciuk and Dick Naslund for providing samples, trace element data, and useful discussions. Thanks to the team at the Pacific Centre for Isotopic and Geochemical Research, particularly Bruno Kieffer, Jane Barling, Richard Friedman, Vivian Lai, and Dejan Milidragovic, for laboratory and analytical assistance. Étienne Girard is thanked for assistance with preparation of the maps. Discussions with Don Francis, Richard Ernst, Jason Coumans, Brian Cousens and Jon Blundy have helped to improve the clarity of our arguments. Nick Arndt, Katie Smart, and Leonid Danyushevsky are thanked for their insightful and thorough reviews. This is NRCan/ESS contribution number #####.

FUNDING

This work was supported by the Geomapping for Energy and Minerals (GEM) program lead by the Geological Survey of Canada and by Natural Science and Engineering Research Council of Canada (NSERC) Discovery Grants to Dominique Weis and James Scoates.

REFERENCES

Ariskin, A. A., Kostitsyn, Y. A., Konnikov, E. G., Danyushevsky, L. V., Meffre, S., Nikolaev, G. S., McNeill, A., Kislov, E. V. & Orsoev, D. A. (2013). Geochronology of the Dovyren intrusive complex, northwestern Baikal area, Russia, in the Neoproterozoic. *Geochemistry International* **51**, 859–875.

Arndt, N., Chauvel, C., Czamanske, G. & Fedorenko, V. (1998). Two mantle sources, two plumbing systems: tholeiitic and alkaline magmatism of the Maymecha River basin, Siberian flood volcanic province. *Contributions to Mineralogy and Petrology* **133**, 297–313.

Arndt, N. T. (1983). Role of a thin, komatiite-rich oceanic crust in the Archean plate-tectonic process. *Geology* **11**, 372–375.

Arndt, N. T. & Christensen, U. (1992). The role of lithospheric mantle in continental flood volcanism: Thermal and geochemical constraints. *Journal of Geophysical Research* **97**, 10967–10981.

Arndt, N. T., Czamanske, G. K., Wooden, J. L. & Fedorenko, V. A. (1993). Mantle and crustal

contributions to continental flood volcanism. *Tectonophysics* **223**, 39–52.

Babinski, M., Van Schmus, W. R. & Chemale Jr., F. (1999). Pb–Pb dating and Pb isotope geochemistry of Neoproterozoic carbonate rocks from the São Francisco basin, Brazil: implications for the mobility of Pb isotopes during tectonism and metamorphism. *Chemical Geology* **160**, 175–199.

Baragar, W. (1976). The Natkusiak Basalts, Victoria Island, District of Franklin. *Geological Survey of Canada Paper* 347–352.

Barling, J., Goldstein, S. L. & Nicholls, I. A. (1994). Geochemistry of Heard Island (Southern Indian Ocean): Characterization of an enriched mantle component and implications for enrichment of the sub-Indian Ocean mantle. *Journal of Petrology* **35**, 1017–1053.

Bédard, J. H. (2005). Partitioning coefficients between olivine and silicate melts. *Lithos* **83**, 394–419.

Bédard, J. H., Hayes, B., Hryciuk, M., Beard, C., Williamson, N., Dell'Oro, T. A., Rainbird, R. H., Prince, J., Baragar, W. R. A., Nabelek, P., Weis, D., Wing, B., Scoates, J. S., Naslund, H. R., Cousens, B., Williamson, M.-C., Hulbert, L. J., Montjoie, R., Girard, É., Ernst, R. & Lissenberg, C. J. (2016). Geochemical database for Victoria Island, Geological Survey of Canada Geomapping for Energy and Minerals project. *Geological Survey of Canada Open File Report 8009* 1 .zip file, doi:10.4095/297842.

Bédard, J. H., Naslund, H. R., Nabelek, P., Winpenny, A., Hryciuk, M., Macdonald, W., Hayes, B., Steigerwaldt, K., Hadlari, T., Rainbird, R., Dewing, K. & Girard, E. (2012). Fault-mediated melt ascent in a Neoproterozoic continental flood basalt province, the Franklin

sills, Victoria Island, Canada. *Geological Society of America Bulletin* **124**, 723–736.

Bédard, J. H., Rainbird, R. H. & Beard, C. (2015). Geology, Qulliq, Victoria Island, Northwest Territories. NTS 87/G01: Geological Survey of Canada.

Black, B. A., Lamarque, J.-F., Shields, C. A., Elkins-Tanton, L. T. & Kiehl, J. T. (2014). Acid rain and ozone depletion from pulsed Siberian Traps magmatism. *Geology* **42**, 67–70.

Bleeker, W. & Ernst, R. (2006). Short-lived mantle generated magmatic events and their dyke swarms: the key unlocking Earth's paleogeographic record back to 2.6 Ga. In: Hanski, E., Mertanen, S., Rämö, T. & Vuollo, J. (eds) *Dyke Swarms–Time Markers of Crustal Evolution*. Rotterdam: A.A. Balkema, 3–26.

Blichert-Toft, J. & Arndt, N. T. (1999). Hf isotope compositions of komatiites. *Earth and Planetary Science Letters* **171**, 439–451.

Bond, D. P. & Wignall, P. B. (2014). Large igneous provinces and mass extinctions: An update. *Geological Society of America Special Papers* **505**, SPE505–02.

Buchan, K. L., Ernst, R., Bleeker, W., Davis, W. J., Villeneuve, M., van Breemen, O., Hamilton, M. A. & Söderlund, U. (2010). Proterozoic magmatic events of the Slave Craton, Wopmay Orogen and environs. *Geological Survey of Canada Open File Report 5985* 1 poster + 25p. report.

Buchan, K. L., Mitchell, R. N., Bleeker, W., Hamilton, M. A. & LeCheminant, A. N. (2016). Paleomagnetism of ca. 2.13–2.11 Ga Indin and ca. 1.885 Ga Ghost dyke swarms of the Slave craton: Implications for the Slave craton APW path and relative drift of Slave,

Superior and Siberian cratons in the Paleoproterozoic. *Precambrian Research* **275**, 151–175.

Campbell, I. H. (2005). Large Igneous Provinces and the mantle plume hypothesis. *Elements* **1**, 265–269.

Campbell, I. H. & Griffiths, R. W. (1990). Implications of mantle plume structure for the evolution of flood basalts. *Earth and Planetary Science Letters* **99**, 79–93.

Carlson, R. W. & Irving, A. J. (1994). Depletion and enrichment history of subcontinental lithospheric mantle: An Os, Sr, Nd and Pb isotopic study of ultramafic xenoliths from the northwestern Wyoming Craton. *Earth and Planetary Science Letters* **126**, 457–472.

Carpentier, M., Weis, D. & Chauvel, C. (2013). Large U loss during weathering of upper continental crust: The sedimentary record. *Chemical Geology* **340**, 91–104.

Chauvel, C., Lewin, E., Carpentier, M., Arndt, N. T. & Marini, J.-C. (2008). Role of recycled oceanic basalt and sediment in generating the Hf–Nd mantle array. *Nature Geoscience* **1**, 64–67.

Connelly, J. N., Ulfbeck, D. G., Thrane, K., Bizzarro, M. & Housh, T. (2006). A method for purifying Lu and Hf for analyses by MC-ICP-MS using TODGA resin. *Chemical Geology* **233**, 126–136.

Courtillot, V. E. & Renne, P. R. (2003). On the ages of flood basalt events. *Comptes Rendus Geoscience* **335**, 113–140.

Cox, G. M., Halverson, G. P., Stevenson, R. K., Vokaty, M., Poirier, A., Kunzmann, M., Li, Z.-

X., Denyszyn, S. W., Strauss, J. V. & Macdonald, F. A. (2016). Continental flood basalt weathering as a trigger for Neoproterozoic Snowball Earth. *Earth and Planetary Science Letters* **446**, 89–99.

Cox, K. G. (1980). A model for flood basalt vulcanism. *Journal of Petrology* **21**, 629–650.

Cox, K. G. & Hawkesworth, C. J. (1984). Relative contribution of crust and mantle to flood basalt magmatism, Mahabaleshwar area, Deccan Traps. *Philosophical Transactions of the Royal Society of London. Series A, Mathematical and Physical Sciences* **310**, 627–641.

Cox, K. G. & Hawkesworth, C. J. (1985). Geochemical stratigraphy of the Deccan Traps at Mahabaleshwar, Western Ghats, India, with implications for open system magmatic processes. *Journal of Petrology* **26**, 355–377.

Davis, W. J., Fryers, B. J. & King, J. E. (1994). Geochemistry and evolution of late Archean plutonism and its significance to the tectonic development of the Slave craton. *Precambrian Research* **67**, 207–241.

Davis, W. J., Gariépy, C. & van Breemen, O. (1996). Pb isotopic composition of late Archaean granites and the extent of recycling early Archaean crust in the Slave Province, northwest Canada. *Chemical Geology* **130**, 255–269.

Davis, W. J. & Hegner, E. (1992). Neodymium isotopic evidence for the tectonic assembly of Late Archean crust in the Slave Province, northwest Canada. *Contributions to Mineralogy and Petrology* **111**, 493–504.

Dell'Oro, T. A. (2012). Sr-Nd-Hf-Pb isotope and trace element geochemistry of the Natkusiak Formation continental flood basalts of the Neoproterozoic Franklin Large Igneous Province. Unpublished MSc Thesis, University of British Columbia, Vancouver, Canada. 193.

Denyszyn, S. W., Halls, H. C., Davis, D. W. & a.D. Evans, D. (2009). Paleomagnetism and U–Pb geochronology of Franklin dykes in High Arctic Canada and Greenland: a revised age and paleomagnetic pole constraining block rotations in the Nares Strait region. *Canadian Journal of Earth Sciences* **46**, 689–705.

DePaolo, D. (1981). Trace element and isotopic effects of combined wallrock assimilation and fractional crystallization. *Earth and Planetary Science Letters* **53**, 189–202.

Dostal, J., Baragar, W. & Dupuy, C. (1986). Petrogenesis of the Natkusiak continental basalts, Victoria Island, Northwest Territories, Canada. *Canadian Journal of Earth Sciences* **23**, 622–632.

Duke, J. M. (1976). Distribution of the period four transition elements among olivine, calcic clinopyroxene and mafic silicate liquid: Experimental results. *Journal of Petrology* **17**, 499–521.

Dupuy, C., Michard, A., Dostal, J., Dautel, D. & Baragar, W. R. A. (1995). Isotope and trace-element geochemistry of Proterozoic Natkusiak flood basalts from the northwestern Canadian Shield. *Chemical Geology* **120**, 15–25.

Egorova, V. & Latypov, R. (2013). Mafic–ultramafic sills: New insights from M- and S-shaped mineral and whole-rock compositional profiles. *Journal of Petrology* **54**, 2155–2191.

Ernst, R. E. (2014). Large Igneous Provinces. Cambridge University Press, Cambridge, UK.

Ernst, R. E. & Buchan, K. L. (2001). The use of mafic dike swarms in identifying and locating mantle plumes. In: Ernst, R. E. & Buchan, K. L. (eds) *Mantle plumes: Their identification through time*. Boulder, Colorado: Geological Society of America, 247–265.

Ewart, A., Milner, S. C., Armstrong, R. A. & Duncan, A. R. (1998). Etendeka volcanism of the Goboboseb Mountains and Messum Igneous Complex, Namibia . Part I : Geochemical evidence of Early Cretaceous Tristan plume melts and the role of crustal contamination in the Etendeka CFB Parana. *Journal of Petrology* **39**, 191–225.

Francis, D. M., Hynes, A. J., Ludden, J. N. & Bédard, J. (1981). Crystal fractionation and partial melting in the petrogenesis of a Proterozoic high-MgO volcanic suite, Ungava, Québec. *Contributions to Mineralogy and Petrology* **78**, 27–36.

Frey, F. A., Weis, D., Borisova, A. Y. & Xu, G. (2002). Involvement of continental crust in the formation of the Cretaceous Kerguelen Plateau: New perspectives from ODP Leg 120 sites. *Journal of Petrology* **43**, 1207–1239.

Gaetani, G. A. & Grove, T. L. (1998). The influence of water on melting of mantle peridotite. *Contributions to Mineralogy and Petrology* **131**, 323–346.

Ganino, C. & Arndt, N. T. (2009). Climate changes caused by degassing of sediments during the emplacement of large igneous provinces. *Geology* **37**, 323–326.

Garfunkel, Z. (2008). Formation of continental flood volcanism — The perspective of setting of melting. *Lithos* **100**, 49–65.

Greene, A. R., Scoates, J. S. & Weis, D. (2008). Wrangellia flood basalts in Alaska: A record of plume-lithosphere interaction in a Late Triassic accreted oceanic plateau. Geochemistry Geophysics Geosystems 9, doi:10.1029/2008GC002092

Greene, A. R., Scoates, J. S., Weis, D., Nixon, G. T. & Kieffer, B. (2009). Melting history and magmatic evolution of basalts and picrites from the accreted Wrangellia oceanic plateau, Vancouver Island, Canada. *Journal of Petrology* **50**, 467–505.

Griselin, M., Arndt, N. T. & Baragar, W. R. A. (1997). Plume-lithosphere interaction and crustal contamination during formation of Coppermine River basalts, Northwest Territories, Canada. *Canadian Journal of Earth Sciences* **34**, 958–975.

Gudfinnsson, G. H. & Presnall, D. C. (2005). Continuous gradations among primary carbonatitic, kimberlitic, melilititic, basaltic, picritic, and komatiitic melts in equilibrium with garnet lherzolite at 3-8 GPa. *Journal of Petrology* **46**, 1645–1659.

Hanano, D., Scoates, J. S. & Weis, D. (2009). Alteration mineralogy and the effect of acid-leaching on the Pb-isotope systematics of ocean-island basalts. *American Mineralogist* **94**, 17–26.

Harris, L. B. (2014). *Structural and tectonic interpretation of geophysical data for NW Victoria Island, Northwest Territories, Canada*. Unpublished initial report prepared for Natural Resources Canada. INRS-ETE, Québec, 35.

Hauri, E. H., Wagner, T. P. & Grove, T. L. (1994). Experimental and natural partitioning of Th, U, Pb and other trace elements between garnet, clinopyroxene and basaltic melts. *Chemical Geology* **117**, 149–166.

Hawkesworth, C., Kelley, S., Turner, S., Le Roex, A. & Storey, B. (1999). Mantle processes during Gondwana break-up and dispersal. *Journal of African Earth Sciences* **28**, 239–261.

Hayes, B., Bédard, J. H., Hryciuk, M., Wing, B., Nabelek, P., MacDonald, W. D. & Lissenberg, C. J. (2015a). Sulfide immiscibility induced by wall-rock assimilation in a fault-guided basaltic feeder system, Franklin Large Igneous Province, Victoria Island (Arctic Canada). *Economic Geology* **110**, 1697–1717.

Hayes, B., Bédard, J. H. & Lissenberg, C. J. (2015b). Olivine slurry replenishment and the development of igneous layering in a Franklin Sill, Victoria Island, Arctic Canada. *Journal of Petrology* **56**, 83–112.

Hayes, B., Lissenberg, C. J., Bédard, J. H. & Beard, C. (2015c). The geochemical effects of olivine slurry replenishment and dolostone assimilation in the plumbing system of the Franklin Large Igneous Province, Victoria Island, Arctic Canada. *Contributions to Mineralogy and Petrology* **169**, 1–18.

He, B., Xu, Y.-G., Chung, S.-L., Xiao, L. & Wang, Y. (2003). Sedimentary evidence for a rapid, kilometer-scale crustal doming prior to the eruption of the Emeishan flood basalts. *Earth and Planetary Science Letters* **213**, 391–405.

Heaman, L. M., LeCheminant, A. N. & Rainbird, R. H. (1992). Nature and timing of Franklin igneous events, Canada: Implications for a Late Proterozoic mantle plume and the break-up of Laurentia. *Earth and Planetary Science Letters* **109**, 117–131.

Heinonen, J. S., Luttinen, A. V. & Bohrson, W. A. (2016). Enriched continental flood basalts

from depleted mantle melts: modeling the lithospheric contamination of Karoo lavas from Antarctica. *Contributions to Mineralogy and Petrology* **171**.

Hergt, J. M., Chappell, B. W., McCulloch, M. T., McDougall, I. & Chivas, A. R. (1989). Geochemical and isotopic constraints on the origin of the Jurassic dolerites of Tasmania. *Journal of Petrology* **30**, 841–883.

Herzberg, C. & Asimow, P. D. (2015). PRIMELT3 MEGA.XLSM software for primary magma calculation: Peridotite primary magma MgO contents from the liquidus to the solidus. Geochemistry Geophysics Geosystems 16, doi:10.1002/2014GC005631

Hirschmann, M. M. & Stolper, E. M. (1996). A possible role for garnet pyroxenite in the origin of the "garnet signature" in MORB. *Contributions to Mineralogy and Petrology* **124**, 185–208.

Hoffman, P. F. & Bowring, S. A. (1984). Short-lived 1.9 Ga continental margin and its destruction, Wopmay orogen, northwest Canada. *Geology* **12**, 68–72.

Hoffman, P. F., Kaufman, A. J., Halverson, G. P. & Schrag, D. P. (1998). A Neoproterozoic Snowball Earth. *Science* **281**, 1342–1346.

Hooper, P. R., Binger, G. B. & Lees, K. R. (2002). Ages of the Steens and Columbia River flood basalts and their relationship to extension-related calc-alkalic volcanism in eastern Oregon. *Geological Society of America Bulletin* **114**, 43–50.

Hooper, P. R. & Hawkesworth, C. J. (1993). Isotopic and Geochemical Constraints on the Origin and Evolution of the Columbia River Basalt. *Journal of Petrology* **34**, 1203–1246.

Horan, M. ., Walker, R., Fedorenko, V. A. & Czamanske, G. K. (1995). Osmium and neodymium isotopic constraints on the temporal and spatial evolution of Siberian flood basalt sources. *Geochimica et Cosmochimica Acta* **59**, 5159–5168.

Hryciuk, M. (2013). Host-rock contamination and sulfide immiscibility in the Franklin Large Igneous Province, Victoria Island, Canada. Unpublished MSc Thesis, McGill University, Montréal, Canada. 177

Huppert, H. E. & Sparks, R. S. J. (1985). Cooling and contamination of mafic and ultramafic magmas during ascent through continental crust. *Earth and Planetary Science Letters* **74**, 371–386.

Huston, D. L., Champion, D. C. & Cassidy, K. F. (2014). Tectonic controls on the endowment of Neoarchean cratons in volcanic-hosted massive sulfide deposits: Evidence from lead and neodymium isotopes. *Economic Geology* **109**, 11–26.

Ingle, S., Weis, D., Doucet, S. & Mattielli, N. (2003). Hf isotope constraints on mantle sources and shallow-level contaminants during Kerguelen hot spot activity since ~120 Ma. Geochemistry, Geophysics, Geosystems 4, doi:10.1029/2002GC000482

Ionov, D. A., Dupuy, C., O'Reilly, S. Y., Kopylova, M. G. & Genshaft, Y. S. (1993). Carbonated peridotite xenoliths from Spitsbergen: implications for trace element signature of mantle carbonate metasomatism. *Earth and Planetary Science Letters* **119**, 283–297.

Jefferson, C. W. (1985). Uppermost Shaler Group and its contact with the Natkusiak basalts, Victoria Island, District of Franklin. *Geological Survey of Canada Current Research* 103–110.

Jefferson, C. W., Nelson, W., Kirkhamr, V., Reedman, J. H. & Scoates, R. F. J. (1985). Geology and copper occurrences of Natkusiak basalts, Victoria Island, District of Franklin. *Geological Survey of Canada Current Research* **85**–**1A**, 203–214.

Jourdan, F., Bertrand, H., Schärer, U., Blichert-Toft, J., Féraud, G. & Kampunzu, A. B. (2007). Major and trace element and Sr, Nd, Hf, and Pb isotope compositions of the Karoo Large Igneous Province, Botswana–Zimbabwe: Lithosphere vs mantle plume contribution. *Journal of Petrology* **48**, 1043–1077.

Kieffer, B., Arndt, N., Lapierre, H., Bastien, F., Bosch, D., Pecher, A., Yirgu, G., Ayalew, D., Weis, D., Jerram, D. A., Keller, F. & Meugniot, C. (2004). Flood and shield basalts from Ethiopia: Magmas from the African superswell. *Journal of Petrology* **45**, 793–834.

Kolebaba, M., Read, G., Kahlert, B. & Kelsch, D. (2003). Diamondiferous kimberlites on Victoria Island, Canada: A northern extension of the Slave Craton. *8th International Kimberlite Conference*, 1–4.

Le Bas, M. J., Le Maitre, R. W., Streckeisen, A. & Zanettin, B. (1986). A chemical classification of volcanic rocks based on the total alkali-silica diagram. *Journal of Petrology* **27**, 745–750.

LeCheminant, A. N. & Heaman, L. M. (1989). Mackenzie igneous events, Canada: Middle Proterozoic hotspot magmatism associated with ocean opening. *Earth and Planetary Science Letters* **96**, 38–48.

Leclerc, F., Bédard, J. H., Harris, L. B., McNicoll, V. J., Goulet, N., Roy, P. & Houle, P. (2011). Tholeiitic to calc-alkaline cyclic volcanism in the Roy Group, Chibougamau area, Abitibi

Greenstone Belt — revised stratigraphy and implications for VHMS exploration. *Canadian Journal of Earth Sciences* **48**, 661–694.

Li, Z., Li, Y., Chen, H., Santosh, M., Yang, S., Xu, Y., Langmuir, C. H., Chen, Z., Yu, X. & Zou, S. (2012). Hf isotopic characteristics of the Tarim Permian large igneous province rocks of NW China: Implication for the magmatic source and evolution. *Journal of Asian Earth Sciences* **49**, 191–202.

Li, Z. X., Bogdanova, S. V., Collins, A. S., Davidson, A., De Waele, B., Ernst, R. E., Fitzsimons, I. C. W., Fuck, R. A., Gladkochub, D. P., Jacobs, J., Karlstrom, K. E., Lu, S., Natapov, L. M., Pease, V., Pisarevsky, S. A., Thrane, K. & Vernikovsky, V. (2008). Assembly, configuration, and break-up history of Rodinia: A synthesis. *Precambrian Research* **160**, 179–210.

Lightfoot, P. C., Hawkesworth, C. J., Hergt, J., Naldrett, A. J., Gorbachev, N. S., Fedorenko, V. A. & Doherty, W. (1993). Remobilisation of the continental lithosphere by a mantle plume: major-, trace-element, and Sr-, Nd-, and Pb-isotope evidence from picritic and tholeiitic lavas of the Noril'sk District, Siberian Trap, Russia. *Contributions to Mineralogy and Petrology* **114**, 171–188.

Lightfoot, P. & Hawkesworth, C. (1988). Origin of Deccan Trap lavas: evidence from combined trace element and Sr-, Nd- and Pb-isotope studies. *Earth and Planetary Science Letters* **91**, 89–104.

Luttinen, A. V., Heinonen, J. S., Kurhila, M., Jourdan, F., Mänttäri, I., Vuori, S. K. & Huhma, H. (2015). Depleted Mantle-sourced CFB Magmatism in the Jurassic Africa–Antarctica Rift:

Petrology and 40Ar/39Ar and U/Pb Chronology of the Vestfjella Dyke Swarm, Dronning Maud Land, Antarctica. *Journal of Petrology* **56**, 919–952.

Macdonald, F. A., Schmitz, M. D., Crowley, J. L., Roots, C. F., Jones, D. S., Maloof, A. C., Strauss, J. V., Cohen, P. A., Johnston, D. T. & Schrag, D. P. (2010). Calibrating the Cryogenian. *Science* **327**, 1241–1243.

Macdonald, G. A. & Katsura, T. (1964). Chemical composition of Hawaiian lavas. *Journal of Petrology* 82–133.

Mackie, R. A., Scoates, J. S. & Weis, D. (2009). Age and Nd–Hf isotopic constraints on the origin of marginal rocks from the Muskox layered intrusion (Nunavut, Canada) and implications for the evolution of the 1.27Ga Mackenzie large igneous province. *Precambrian Research* **172**, 46–66.

Malitch, K. N., Belousova, E. A., Griffin, W. L. & Badanina, I. Y. (2013). Hafnium-neodymium constraints on source heterogeneity of the economic ultramafic-mafic Noril'sk-1 intrusion (Russia). *Lithos* **164–167**, 36–46.

Malitch, K. N., Belousova, E. A., Griffin, W. L., Badanina, I. Y., Pearson, N. J., Presnyakov, S. L. & Tuganova, E. V. (2009). Magmatic evolution of the ultramafic–mafic Kharaelakh intrusion (Siberian Craton, Russia): insights from trace-element, U–Pb and Hf-isotope data on zircon. *Contributions to Mineralogy and Petrology* **159**, 753–768.

Marsh, B. D. (2004). A magmatic mush column rosetta stone: The McMurdo Dry Valleys of Antarctica. *Eos, Transactions American Geophysical Union* **85**, 497.

McDonald, I. & Viljoen, K. S. (2006). Platinum-group element geochemistry of mantle eclogites: a reconnaissance study of xenoliths from the Orapa kimberlite, Botswana. *Applied Earth Science* **115**, 81–93.

McDonough, W. F. & Sun, S.-S. (1995). The composition of the Earth. *Chemical Geology* **120**, 223–253.

McKenzie, D. (1989). Some remarks on the movement of small melt fractions in the mantle. *Earth and Planetary Science Letters* **95**, 53–72.

Mysen, B. O. & Boettcher, A. L. (1975). Melting of a hydrous mantle: I. Phase relations of natural peridotite at high pressures and temperatures with controlled activities of water, carbon dioxide, and hydrogen. *Journal of Petrology* **16**, 520–548.

Nabelek, P. I., Bédard, J. H., Hryciuk, M. & Hayes, B. (2012). Short-duration contact metamorphism of calcareous sedimentary rocks by Neoproterozoic Franklin gabbro sills and dikes on Victoria Island, Canada. *Journal of Metamorphic Geology* 205–220.

Neill, I., Kerr, A. C., Hastie, A. R., Pindell, J. L. & Millar, I. L. (2013). The Albian-Turonian island arc rocks of Tobago, West Indies: Geochemistry, petrogenesis, and Caribbean plate tectonics. *Journal of Petrology* **54**, 1607–1639.

Nobre Silva, I. G., Weis, D., Barling, J. & Scoates, J. S. (2009). Leaching systematics and matrix elimination for the determination of high-precision Pb isotope compositions of ocean island basalts. Geochemistry Geophysics Geosystems 10, doi:10.1029/2009GC002537

Nobre Silva, I. G., Weis, D. & Scoates, J. S. (2010). Effects of acid leaching on the Sr-Nd-Hf

isotopic compositions of ocean island basalts. Geochemistry Geophysics Geosystems 11, Q09011. doi:10.1029/2010GC003176

Nowell, G. M., Pearson, D. G., Bell, D. R., Carlson, R. W., Smith, C. B., Kempton, P. D. & Noble, S. R. (2004). Hf isotope systematics of kimberlites and their megacrysts: New constraints on their source regions. *Journal of Petrology* **45**, 1583–1612.

Ochs, F. A. & Lange, R. A. (1999). The density of hydrous magmatic liquids. *Science* **283**, 1314–1317.

O'Hara, M. J. & Mathews, R. E. (1981). Geochemical evolution in an advancing, periodically replenished, periodically tapped, continuously fractionated magma chamber. *Journal of the Geological Society* **138**, 237–277.

Pearce, J. A. (2008). Geochemical fingerprinting of oceanic basalts with applications to ophiolite classification and the search for Archean oceanic crust. *Lithos* **100**, 14–48.

Pearce, J. A. & Norry, M. J. (1979). Petrogenetic implications of Ti, Zr, Y, and Nb variations in volcanic rocks. *Contributions to Mineralogy and Petrology* **69**, 33–47.

Pehrsson, S. J. & Buchan, K. L. (1999). Borden dykes of Baffin Island, Northwest Territories: a Franklin U–Pb baddeleyite age and a paleomagnetic reinterpretation. *Canadian Journal of Earth Sciences* **36**, 65–73.

Pretorius, W., Weis, D., Williams, G., Hanano, D., Kieffer, B. & Scoates, J. (2006). Complete trace elemental characterisation of granitoid (USGS G-2, GSP-2) reference materials by high resolution inductively coupled plasma-mass spectrometry. *Geostandards and*

Geoanalytical Research **30**, 39–54.

Rainbird, R. H. (1993). The sedimentary record of mantle plume uplift preceding eruption of the Neoproterozoic Natkusiak flood basalt. *The Journal of Geology* **101**, 305–318.

Rainbird, R. H., Jefferson, C. W., Hildebrand, R. S. & Worth, J. K. (1994). The Shaler Supergroup and revision of Neoproterozoic stratigraphy in Amundsen Basin, Northwest Territories. *Geological Survey of Canada Current Research* **1994–C**, 61–70.

Rapp, R. P. & Watson, E. B. (1995). Dehydration melting of metabasalt at 8–32 kbar: Implications for continental growth and crust-mantle recycling. *Journal of Petrology* **36**, 891–931.

Renne, P. R., Deckart, K., Ernesto, M., Fe´raud, G. & Piccirillo, E. M. (1996). Age of the Ponta Grossa dike swarm (Brazil), and implications to Parana´flood volcanism. *Earth and Planetary Science Letters* **144**, 199–211.

Richards, M. A., Jones, D. L., Duncan, R. A. & Depaolo, D. J. (1991). A mantle plume initiation model for the Wrangellia flood basalt and other oceanic plateaus. *Science* **254**, 263–267.

Rubatto, D. & Hermann, J. (2007). Experimental zircon/melt and zircon/garnet trace element partitioning and implications for the geochronology of crustal rocks. *Chemical Geology* **241**, 38–61.

Rudnick, R. L. & Gao, S. (2003). Composition of the continental crust. In: Holland, H. D. & Turekian, K. K. (eds) *Treatise on Geochemistry*. Oxford: Pergamon, 1–64.

Salters, V. J. M. & Stracke, A. (2004). Composition of the depleted mantle. Geochemistry

Geophysics Geosystems 5, Q05B07, doi:10.1029/2003GC000597

Schmidberger, S. S., Heaman, L. M., Simonetti, A., Creaser, R. A. & Cookenboo, H. O. (2005). Formation of Paleoproterozoic eclogitic mantle, Slave Province (Canada): Insights from in-situ Hf and U–Pb isotopic analyses of mantle zircons. *Earth and Planetary Science Letters* **240**, 621–633.

Schmidberger, S. S., Simonetti, A., Francis, D. & Gariépy, C. (2002). Probing Archean lithosphere using the Lu–Hf isotope systematics of peridotite xenoliths from Somerset Island kimberlites, Canada. *Earth and Planetary Science Letters* **197**, 245–259.

Schmidberger, S. S., Simonetti, A., Heaman, L. M., Creaser, R. A. & Whiteford, S. (2007). Lu–Hf, in-situ Sr and Pb isotope and trace element systematics for mantle eclogites from the Diavik diamond mine: Evidence for Paleoproterozoic subduction beneath the Slave craton, Canada. *Earth and Planetary Science Letters* **254**, 55–68.

Schudel, G., Lai, V., Gordon, K. & Weis, D. (2015). Trace element characterization of USGS reference materials by HR-ICP-MS and Q-ICP-MS. *Chemical Geology* **410**, 223–236.

Shellnutt, J. G., Dostal, J. & Keppie, J. D. (2004). Petrogenesis of the 723 Ma Coronation sills, Amundsen basin, Arctic Canada: implications for the break-up of Rodinia. *Precambrian Research* **129**, 309–324.

Smart, K. A., Chacko, T., Simonetti, A., Sharp, Z. D. & Heaman, L. M. (2014). A record of Paleoproterozoic subduction preserved in the Northern Slave cratonic mantle: Sr–Pb–O isotope and trace-element investigations of eclogite xenoliths from the Jericho and Muskox kimberlites. *Journal of Petrology* **55**, 549–583.

Smart, K. A., Heaman, L. M., Chacko, T., Simonetti, A., Kopylova, M., Mah, D. & Daniels, D. (2009). The origin of high-MgO diamond eclogites from the Jericho Kimberlite, Canada. *Earth and Planetary Science Letters* **284**, 527–537.

Sobolev, A. V., Krivolutskaya, N. A. & Kuzmin, D. V. (2009). Petrology of the parental melts and mantle sources of Siberian trap magmatism. *Petrology* **17**, 253–286.

Sobolev, S. V., Sobolev, A. V., Kuzmin, D. V., Krivolutskaya, N. A., Petrunin, A. G., Arndt, N. T., Radko, V. A. & Vasiliev, Y. R. (2011). Linking mantle plumes, large igneous provinces and environmental catastrophes. *Nature* **477**, 312–6.

Spera, F. J. & Bohrson, W. A. (2001). Energy-constrained open-system magmatic processes I: General model and energy-constrained assimilation and fractional crystallization (EC-AFC) formulation. *Journal of Petrology* **42**, 999–1018.

Stacey, J. t & Kramers, 1JD (1975). Approximation of terrestrial lead isotope evolution by a two-stage model. *Earth and Planetary Science Letters* **26**, 207–221.

Storey, M., Duncan, R. A. & Tegner, C. (2007). Timing and duration of volcanism in the North Atlantic Igneous Province: Implications for geodynamics and links to the Iceland hotspot. *Chemical Geology* **241**, 264–281.

Storey, M., Mahoney, J. J., Kroenke, L. W. & Saunders, A. D. (1991). Are oceanic plateaus sites of komatiite formation? *Geology* **19**, 376–379.

Stracke, A., Bizimis, M. & Salters, V. J. M. (2003). Recycling oceanic crust: Quantitative constraints. *Geochemistry, Geophysics, Geosystems* **4**, 8003.

Sun, S. S. & McDonough, W. F. (1989). Chemical and isotopic systematics of oceanic basalts: implications for mantle composition and processes. *Geological Society, London, Special Publications* **42**, 313–345.

Tejada, M. L. G., Mahoney, J. J., Castillo, P. R., Ingle, S. P., Sheth, H. C. & Weis, D. (2004). Pin-pricking the elephant: evidence on the origin of the Ontong Java Plateau from Pb-Sr-Hf-Nd isotopic characteristics of ODP Leg 192 basalts. *Geological Society, London, Special Publications* **229**, 133–150.

Thomson, D., Rainbird, R. H., Planavsky, N., Lyons, T. W. & Bekker, A. (2015). Chemostratigraphy of the Shaler Supergroup, Victoria Island, NW Canada: A record of ocean composition prior to the Cryogenian glaciations. *Precambrian Research* **263**, 232–245.

Thorpe, R. I., Cumming, G. L. & Mortensen, J. K. (1992). Pb-isotope boundary in the Slave Province and its probable relation to ancient basement in the western Slave. *Geological Survey of Canada Open File Report 2484* 261.

Thorsteinsson, R. & Tozer, E. T. (1962). Banks, Victoria and Stefansson Islands, Arctic Archipelago. *Geological Survey of Canada Memoir* 85p.

Tiepolo, M., Bottazzi, P., Foley, S. F., Oberti, R., Vannucci, R. & Zanetti, A. (2001). Fractionation of Nb and Ta from Zr and Hf at mantle depths: the role of titanian pargasite and kaersutite. *Journal of Petrology* **42**, 221–232.

Turner, S. & Hawkesworth, C. (1995). The nature of the sub-continental mantle: constraints from the major-element composition of continental flood basalts. *Chemical Geology* **120**, 295–

314.

Turner, S. J. & Langmuir, C. H. (2015). The global chemical systematics of arc front stratovolcanoes: Evaluating the role of crustal processes. *Earth and Planetary Science Letters* **422**, 182–193.

Vanderkluysen, L., Mahoney, J. J., Hooper, P. R., Sheth, H. C. & Ray, R. (2011). The feeder system of the Deccan Traps (India): Insights from dike geochemistry. *Journal of Petrology* **52**, 315–343.

Varfalvy, V., Hebert, R., Bedard, J. H. & Lafleche, M. R. (1997). Petrology and geochemistry of pyroxenite dykes in upper mantle peridotites of the North Arm Mountain massif, Bay of Islands ophiolite, Newfoundland: implications for the genesis of boninitic and related magmas. *Canadian Mineralogist* **35**, 543–570.

Vervoort, J. D. & Blichert-Toft, J. (1999). Evolution of the depleted mantle: Hf isotope evidence from juvenile rocks through time. *Geochimica et Cosmochimica Acta* **63**, 533–556.

Vervoort, J. D. & Jonathan Patchett, P. (1996). Behavior of hafnium and neodymium isotopes in the crust: Constraints from Precambrian crustally derived granites. *Geochimica et Cosmochimica Acta* **60**, 3717–3733.

Vervoort, J. D., Patchett, P. J., Albarède, F., Blichert-Toft, J., Rudnick, R. & Downes, H. (2000). Hf–Nd isotopic evolution of the lower crust. *Earth and Planetary Science Letters* **181**, 115–129.

Vervoort, J. D., Patchett, P. J., Blichert-Toft, J. & Albarède, F. (1999). Relationships between

Lu–Hf and Sm–Nd isotopic systems in the global sedimentary system. *Earth and Planetary Science Letters* **168**, 79–99.

Weis, D., Garcia, M. O., Rhodes, J. M., Jellinek, M. & Scoates, J. S. (2011). Role of the deep mantle in generating the compositional asymmetry of the Hawaiian mantle plume. *Nature Geoscience* **4**, 831–838.

Weis, D., Kieffer, B., Hanano, D., Nobre Silva, I., Barling, J., Pretorius, W., Maerschalk, C. & Mattielli, N. (2007). Hf isotope compositions of U.S. Geological Survey reference materials. Geochemistry Geophysics Geosystems 8. doi:10.1029/2006GC001473

Weis, D., Kieffer, B., Maerschalk, C., Barling, J., de Jong, J., Williams, G. a., Hanano, D., Pretorius, W., Mattielli, N., Scoates, J. S., Goolaerts, A., Friedman, R. M. & Mahoney, J. B. (2006). High-precision isotopic characterization of USGS reference materials by TIMS and MC-ICP-MS. Geochemistry Geophysics Geosystems 7. doi:10.1029/2006GC001283

Weis, D., Kieffer, B., Maerschalk, C., Pretorius, W. & Barling, J. (2005). High-precision Pb-Sr-Nd-Hf isotopic characterization of USGS BHVO-1 and BHVO-2 reference materials. Geochemistry Geophysics Geosystems 6, Q02002, doi:10.1029/2004GC000852

White, R. & McKenzie, D. (1989). Magmatism at rift zones: The generation of volcanic continental margins and flood basalts. *Journal of Geophysical Research* **94**, 7685–7729.

White, W. M. (2010). Oceanic island basalts and mantle plumes: The geochemical perspective. *Annual Review of Earth and Planetary Sciences* **38**, 133–160.

Willbold, M. & Stracke, A. (2006). Trace element composition of mantle end-members: Implications for recycling of oceanic and upper and lower continental crust. *Geochemistry Geophysics Geosystems* **7**, 1–30.

Willbold, M. & Stracke, A. (2010). Formation of enriched mantle components by recycling of upper and lower continental crust. *Chemical Geology* **276**, 188–197.

Williamson, N., Bédard, J. H., Ootes, L., Rainbird, R. H., Cousens, B. & Zagorevski, A. (2013). Volcanostratigraphy and significance of the southern lobe Natkusiak Formation flood basalts, Victoria Island, Northwest Territories. *Geological Survey of Canada Current Research* **2013–16**, 15.

Williamson, N. M. B., Ootes, L., Rainbird, R. H., Bédard, J. H. & Cousens, B. (2016). Initiation and early evolution of the Franklin magmatic event preserved in the 720 Ma Natkusiak Formation, Victoria Island, Canadian Arctic. *Bulletin of Volcanology* **78**, 1–19.

Wood, D. A. (1980). The application of a Th–Hf–Ta diagram to problems of tectonomagmatic classification and to establishing the nature of crustal contamination of basaltic lavas of the British Tertiary Volcanic Province. *Earth and Planetary Science Letters* **50**, 11–30.

Wooden, J. L., Czamanske, G. K., Fedorenko, V. A., Arndt, N. T., Chauvel, C., Bouse, R. M., King, B.-S. W., Knight, R. J. & Siems, D. F. (1993). Isotopic and trace-element constraints on mantle and crustal contributions to Siberian continental flood basalts, Noril'sk area, Siberia. *Geochimica et Cosmochimica Acta* **57**, 3677–3704.

Wright, I. P., Hartmetz, C. P. & Pillinger, C. T. (1993). An assessment of the nature and origins of the carbon-bearing components in fines collected during the sawing of EET A79001.

Journal of Geophysical Research **98**, 3477–3482.

Xie, Q., Kerrich, R. & Fan, J. (1993). HFSE/REE fractionations recorded in three komatiite-basalt sequences, Archean Abitibi greenstone belt: Implications for multiple plume sources and depths. *Geochimica et Cosmochimica Acta* **57**, 4111–4118.

Yamashita, K., Creaser, R. A., Stemler, J. U. & Zimaro, T. W. (1999). Geochemical and Nd–Pb isotopic systematics of late Archean granitoids, southwestern Slave Province, Canada: constraints for granitoid origin and crustal isotopic structure. *Canadian Journal of Earth Sciences* **36**, 1131–1147.

Yaxley, G. M. (2000). Experimental study of the phase and melting relations of homogeneous basalt + peridotite mixtures and implications for the petrogenesis of flood basalts. *Contributions to Mineralogy and Petrology* **139**, 326–338.

Zartman, R. E. & Doe, B. R. (1981). Plumbotectonics—the model. *Tectonophysics* **75**, 135–162.

Zhang, H.-F., Goldstein, S. L., Zhou, X.-H., Sun, M., Zheng, J.-P. & Cai, Y. (2008). Evolution of subcontinental lithospheric mantle beneath eastern China: Re–Os isotopic evidence from mantle xenoliths in Paleozoic kimberlites and Mesozoic basalts. *Contributions to Mineralogy and Petrology* **155**, 271–293.

Zindler, A. & Hart, S. (1986). Chemical geodynamics. *Annual Review of Earth and Planetary Sciences* **14**, 493–571.

FIGURE CAPTIONS

Fig. 1. Map of Arctic Canada and Greenland indicating the position of the Franklin dykes (red), sills (green), and the coeval Natkusiak Formation flood basalts (black), modified after Buchan *et al.* (2010). Greenland is relocated to its pre-drift position relative to the North American continent based on sea floor magnetic anomalies. The star indicates the inferred locus of magmatic upwelling and is based on the orientation of the dykes. The inset map shows the extent of the Franklin magmatism overlain on continents restored to 720 Ma positions and is modified after Cox *et al.* (2016). NS is the North Slope subterrane of Arctic Alaska, MN is Mongolia, and GN is the 780 Ma Gunbarrel dykes, which are exposed in western North America.

Fig. 2. Geology of the Franklin large igneous province on Victoria Island, Arctic Canada. (a) Simplified geological map of Victoria Island modified from Bédard *et al.* (2012) with regional location in Northern Canada highlighted in the inset in the upper left. Note that Franklin sills are emplaced throughout the Shaler Supergroup and individual intrusive bodies are omitted for clarity. The studied volcanic sections in the Natkusiak Formation basalts are indicated as black stars (e.g. West Section, Central Section) and relevant sill localities are shown. Type 1 sills are labelled by name: LPS is Lower Pyramid Sill; WUS is the West Uhuk Sill. (b) Detailed geological map in the area of the Minto Inlet showing the lateral continuity of the Franklin sills (purple unit = Franklin Gabbro). Modified from Bédard *et al.* (2015) and other maps in the series.

Fig. 3. Photographs showing contact relations and internal structure of the Natkusiak basalts and Franklin sills on Victoria Island. (a) Cliff exposure of the laterally continuous contact between the Kuujjua sandstone (sst) and basal Natkusiak basalts on the south side of the Kuujjua River valley, west of the central section. Image facing southwest, with vertical section of cliff approximately 100 m in height. (b) Detail of the same cliff section, illustrating the sharpness of

the contact between the Kuujjua sandstone and the basal Natkusiak basalts, vertical scale approx. 100 m. (c) Cliff exposure showing rare lobes of Kuujjua sandstone interbedded with the basal Natkusiak basalts, indicating that fluvial deposition continued after the initiation of volcanism (Rainbird, 1993). Image from the northeastern edge of the southern lobe of the Natkusiak basalts, facing eastward, vertical exposure approximately 70 m. (d) The Pyramid sills (Hayes *et al.*, 2015b, 2015c), photographed from a helicopter above the Minto Inlet, facing northwest. The Lower Pyramid sill is a 20 m thick Type 1 sill, and the top of the Upper Pyramid sill is approximately 250 m above sea level. (e) Cliff exposures of Type 2 Franklin sills on the southern shore of the Minto Inlet, taken from a helicopter, facing northeast. Cliffs <15 m in height. (f) Laterally continuous Type 2 Franklin sills with sharp contacts, taken from a helicopter facing southeast across the Kuujjua River valley, cliffs approximately 120 m total height. (g) A typical basal contact of a Type 2 sill near the community of Ulukhaktok. The margin of the sill is chilled against the host Kilian Formation sulphate evaporites, which display only localised alteration (<10 cm). Hammer handle length is one meter. (h) An olivine-rich horizon from the base of the West Uhuk sill, displaying a characteristic 'elephant skin' weathering texture. Hammer handle diameter is 4.5 cm.

Fig. 4. Stratigraphic variation in whole rock geochemistry from four sections of the Natkusiak basalts. Major element oxide compositions from Williamson *et al.* (2016). The absolute stratigraphic position of the East and West sections, which contain only V1 lavas, are not known (Dell'Oro, 2012). For the West Section samples, heights are shown relative to the base of Unit V_1 (sheet flow basalts). See Figure 2 for field locations. Abbreviations in stratigraphic column: x bed Vclastic = cross-bedded volcaniclastic deposits; Wthred Unit = weathered unit.

Fig. 5. Major element oxide variation diagrams for whole-rocks of the Natkusiak basalts and Franklin sills on Victoria Island. Fields for Type 1 and Type 2 rocks from the complete Victoria Island geochemical database (Bédard *et al.*, 2016) are outlined with dashed lines. In (a), the alkali discriminant line is from Macdonald & Katsura (1964) and the volcanic classification fields are from Le Bas *et al.* (1986). Oxides are plotted on an anhydrous, normalized basis with total iron expressed as FeO. Mid-ocean ridge basalt (MORB) and depleted mantle (DM) compositions are from Salters & Stracke (2004), and upper crust (UC), middle crust (MC) and lower continental crust (LC) compositions are from Rudnick & Gao (2003). Hand-drawn dashed lines surrounding the full VI database are for clarity and contain >95 % of the samples; most of the rocks that lie outside of these dashed lines are altered. Note the strong olivine control line defined by the high-MgO whole-rock compositions from the Type 1 sills.

Fig. 6. Trace element variation diagrams for whole-rocks of the Natkusiak basalts and Franklin sills on Victoria Island. Results for the Coronation sills (Shellnutt *et al.*, 2004) are plotted for comparison. Fields for Type 1 and Type 2 rocks from the complete Victoria Island geochemical database (Bédard *et al.*, 2016) are outlined with hand-drawn dashed lines. Mid-ocean ridge basalt (MORB) and depleted mantle (DM) compositions are from Salters & Stracke (2004), and upper crust (UC), middle crust (MC) and lower continental crust (LC) compositions are from Rudnick & Gao (2003). Analyses of whole rocks from the Shaler Supergroup from Victoria Island are plotted for comparison. Analytical reproducibility is at the 2σ level and was determined by repeat analyses of the USGS reference material BCR-2 (Schudel *et al.*, 2015).

Fig. 7. Normalised trace element variation diagrams for whole rocks of the Natkusiak basalts and Franklin sills on Victoria Island. (a) Primitive mantle-normalised extended trace element patterns, with primitive mantle-normalising values from Sun & McDonough (1989). (b)

Chondrite-normalised rare earth element patterns, with chondrite-normalising values from McDonough & Sun (1995). Solid lines show the compositions of individual samples of Natkusiak basalt, whereas the shaded fields indicate the range of compositions present in the Franklin sills. Dashed lines show model compositions for incongruent dynamic melts of a mixed source of garnet lherzolite and spinel lherzolite and are from Greene *et al.* (2009, their Fig. 14b).

Fig. 8. Initial ε_{Nd} and $^{87}Sr/^{86}Sr$ for whole-rocks of Natkusiak basalts and Franklin sills on Victoria Island. Results for the Coronation sills (Shellnutt *et al.*, 2004) are plotted for comparison and have been re-corrected for age from the original reported results. Fields showing ocean island basalt compositions are from Willbold & Stracke (2010) and include EM-I (enriched mantle-I), EM-II (enriched mantle-II), and HIMU (high μ, or high $^{238}U/^{204}Pb$). These have been age corrected to 723 Ma isotopic compositions using source compositions from Stracke *et al.* (2003) for HIMU and Willbold & Stracke (2006) for EM-I and EM-II compositions. Depleted mantle and extreme depleted mantle compositions are from Salters & Stracke (2004). Dashed lines represent CHUR (ε_{Nd}) and UR ($^{87}Sr/^{86}Sr$).

Fig. 9. Ce/Yb, initial ε_{Nd} and initial ε_{Hf} diagrams for whole-rocks of Natkusiak basalts and Franklin sills on Victoria Island. Results for the coeval Coronation sills on the Canadian mainland (Shellnutt *et al.*, 2004) are plotted for comparison and have been re-corrected for age from the original reported results. Depleted MORB (DM) and MORB compositions as defined in Figure 8. The terrestrial array (long-dashed line) in (b) is from Vervoort *et al.*, (1999) and the short-dashed lines indicate the approximate range of oceanic basalts. Black and grey bold lines show the isotopic evolution of mafic Archean and Palaeoproterozoic rocks of suggested oceanic origin, with (i) as initial compositions, and marked ticks at 1 Ga incubation intervals (model after

Nowell *et al.*, 2004). The Munro-type komatiites are from the Abitibi and Belingwe belts (n = 5), the Barberton komatiites are from the Barberton belt (n = 3, both Blichert-Toft & Arndt, 1999), the Abitibi basaltic andesite is indicated "B-A", and the Cape Smith belt basalts (n = 7) are from the Chukotat Group (both Vervoort & Blichert-Toft, 1999). The model suggests that the source of the Southern Natkusiak basalts may include an isotopically matured Munro-type komatiite component, and discounts major involvement of Abitibi-type basaltic andesite or Barberton-type komatiite.

Fig. 10. Initial Pb isotope compositions for whole-rocks of the Natkusiak basalts and Franklin sills on Victoria Island. (a) initial $^{206}Pb/^{206}Pb$ vs. $^{207}Pb/^{204}Pb$. (b) initial $^{206}Pb/^{204}Pb$ vs. $^{208}Pb/^{204}Pb$. The age-corrected ocean island basalt compositions from Willbold & Stracke (2010) are plotted for comparison (EM-I, EM-II, HIMU, age corrections as in Figure 8). M = mantle, Or = Orogene, UC = upper continental crust, LC = lower continental crust (all from Zartman & Doe, 1981, age corrected to 723 Ma). The mixing lines show the relative compositional effect of assimilating rocks from the Shaler Supergroup, with yellow filled circles representing the average Type 1 sill composition and tick marks labelled with percentage contributions from sedimentary rocks. See Hayes *et al.* (2015c) for detailed discussion.

Fig. 11. Diagrams showing the spatial variations in initial ε_{Nd} for whole-rocks of Natkusiak basalts and Franklin sills on Victoria Island. (a) Latitude (degrees north) vs. initial ε_{Nd}. (b) Longitude (degrees west) vs. initial ε_{Nd}. The Nd isotope compositions of the Type 2 basalts are correlated with geographic position, a trend that is not observed for the Franklin sills.

Fig. 12. Trace element ratio diagrams for whole-rocks of the Natkusiak basalts and Franklin sills on Victoria Island used to evaluate crustal input, melting depth, and source

composition (Pearce, 2008). (a) Th/Yb vs. Nb/Yb. All samples from the Franklin LIP plot above the MORB-OIB array of Pearce (2008) and are consistent with the incorporation of continental material in the basaltic magmas. (b) TiO_2/Yb vs. Nb/Yb. The samples from the Franklin LIP plot on the boundary between the deep (OIB) and shallow (MORB) melting arrays of Pearce (2008). Abbreviations: DMM – depleted MORB mantle; N-MORB – normal mid-ocean ridge basalt; E-MORB – enriched mid-ocean ridge basalt; OIB – ocean island basalt (DMM, N-MORB, E-MORB, OIB from Pearce, 2008); LC – lower continental crust; MC – middle continental crust; UC – upper continental crust (compositions from Rudnick & Gao, 2003). In (a), the representative Shaler Supergroup host-rocks have compositions similar to middle continental crust, and overlap with the volcanic arc array.

Fig. 13. Trace element ratio and Nd isotope diagrams for whole-rocks of the Natkusiak basalts and Franklin sills on Victoria Island showing calculated bulk mixtures of Type 1 and Type 2 primary melts in equilibrium with Fo_{90} olivine and a mixture of Slave Province granitoids. Primary melt compositions are calculated back to Fo_{90} equilibrium compositions by incrementally adding equilibrium olivine (Turner & Langmuir, 2015). The curves are marked at 5% intervals (small crosses). For comparison, a variety of rock types are plotted, including Coronation sills (Shellnutt *et al.*, 2004), and Slave Province granitoids (Davis *et al.*, 1994; Yamashita *et al.*, 1999). The MORB-OIB field in (d) is from Pearce (2008). The MORB and continental crustal compositions are as defined in Figure 6.

Fig. 14. Variation of Nb/La with respect to initial ε_{Nd}, SiO_2, CaO/Al_2O_3 and Zr for whole-rocks of the Natkusiak basalts and Franklin sills on Victoria Island. There is a positive correlation between Nb/La and initial ε_{Nd} in the Franklin sills, however, the correlation is weaker

with major element oxide and trace element indices that are affected by fractional crystallisation (i.e. plagioclase accumulation and fractionation). This suggests that Nb/La was not controlled by fractional crystallisation and thus largely reflect changes in source chemistry and contamination. Also shown is the mixing model from Fig. 13.

Fig. 15. Schematic cross-sections showing the intrusion pathways and distribution of source components associated with Franklin magmatism on Victoria Island. Panel (a) shows early development of the Franklin LIP in which Type 1 sills were emplaced and the Northern and Southern Type 1 Natkusiak flood basalts were erupted. As Southern Type 1 magmas show no continental geochemical influence, we suggest that they likely transgressed rapidly through the crust. Northern Type 1 magmas were probably less buoyant, hence formed an extensive intrusive complex, which extends below the Southern Type 1 basalts. Extension associated with thermal doming and uplift in the north may have aided the development of magma pathways and promoted eruption of the basal flood basalts in the north, despite their lower buoyancy. Panel (b) shows the Franklin LIP in its zenith of activity, with emplacement of the extensive Type 2 sill complex and voluminous outpourings of sheet flow basalts in the north and south. Note how the sheet flow basalts record a continuum in Nd isotopic compositions, with more positive initial ε_{Nd} to the south, whilst all the Type 2 sills have initial ε_{Nd} that match the northern section sheet flow basalts. Horizontal field of view is approximately 200 km.

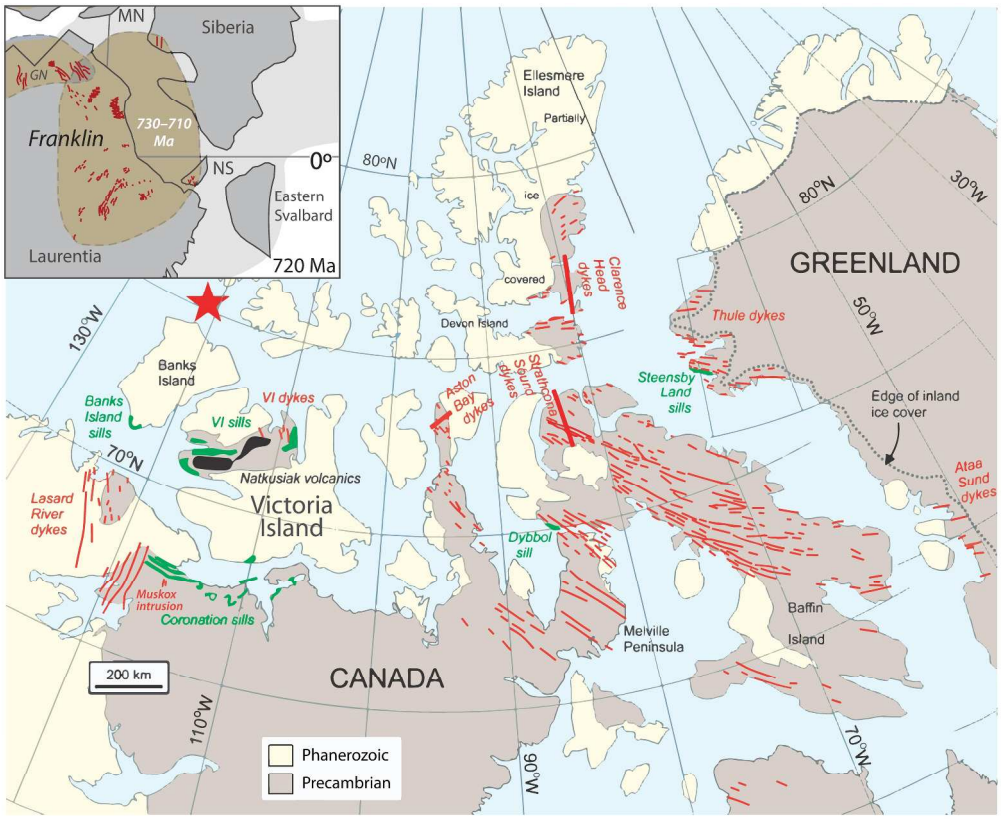

Figure 1. Regional maps showing the extent of the Franklin LIP

270x233mm (300 x 300 DPI)

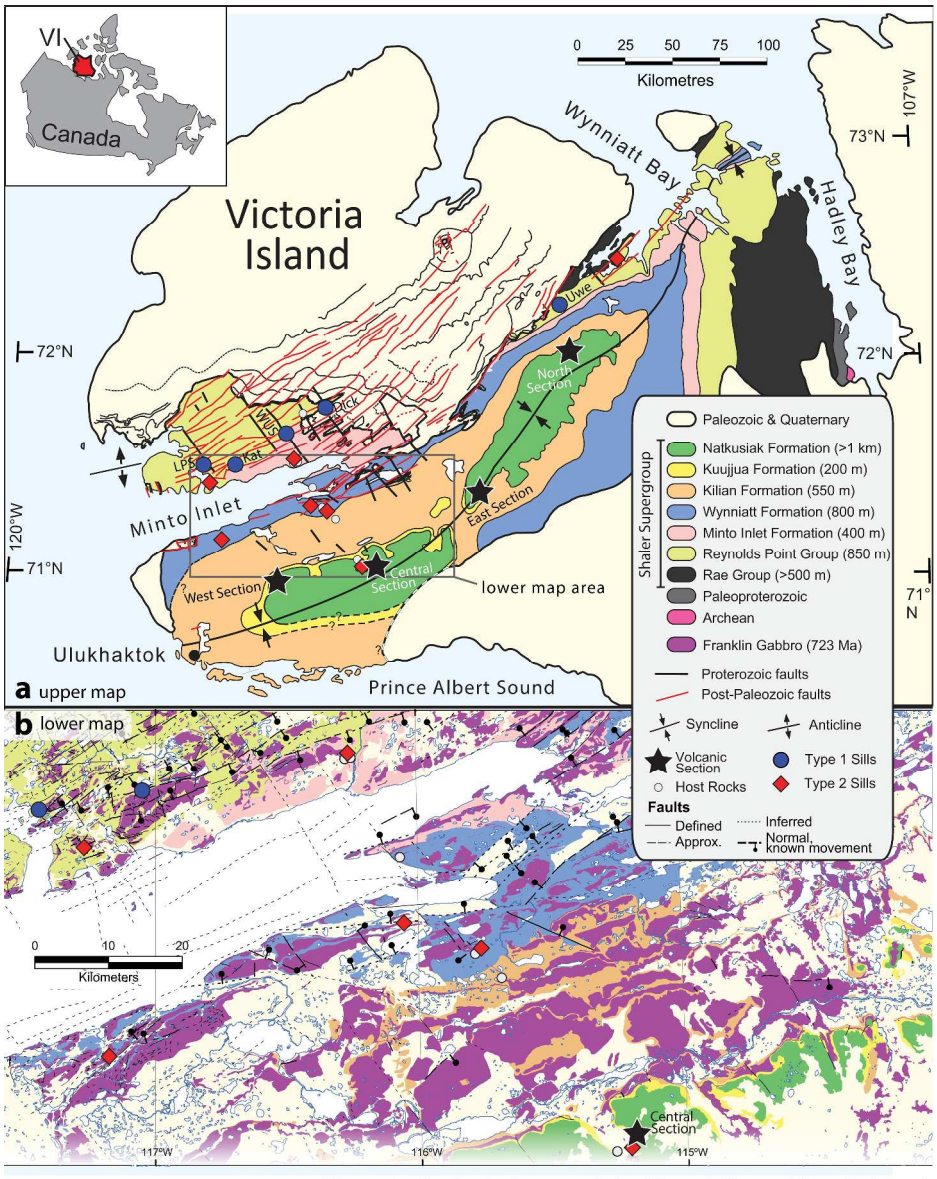

Figure 2. Geological maps of the Minto Inlier on Victoria Island

468x605mm (300 x 300 DPI)

Figure 3. Photographs of the Natkusiak basalts and Franklin sills on Victoria Island

360x389mm (300 x 300 DPI)

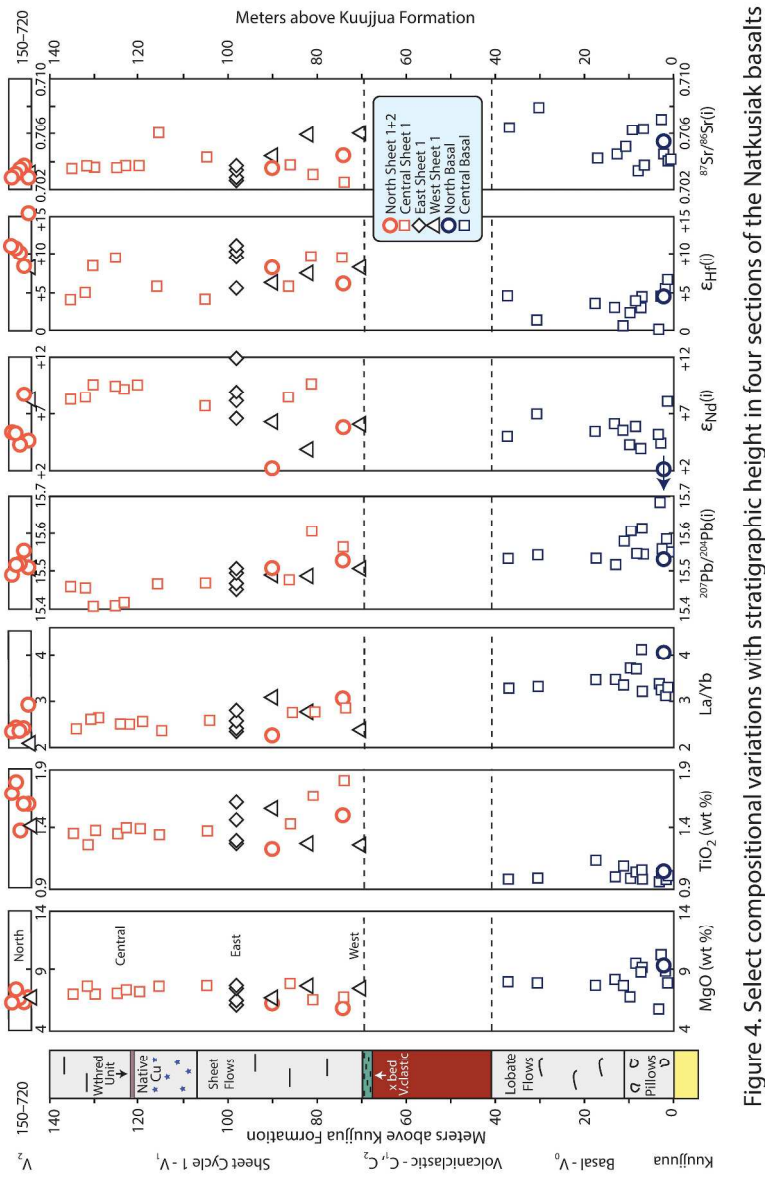

Figure 4. Select compositional variations with stratigraphic height in four sections of the Natkusiak basalts

286x440mm (300 x 300 DPI)

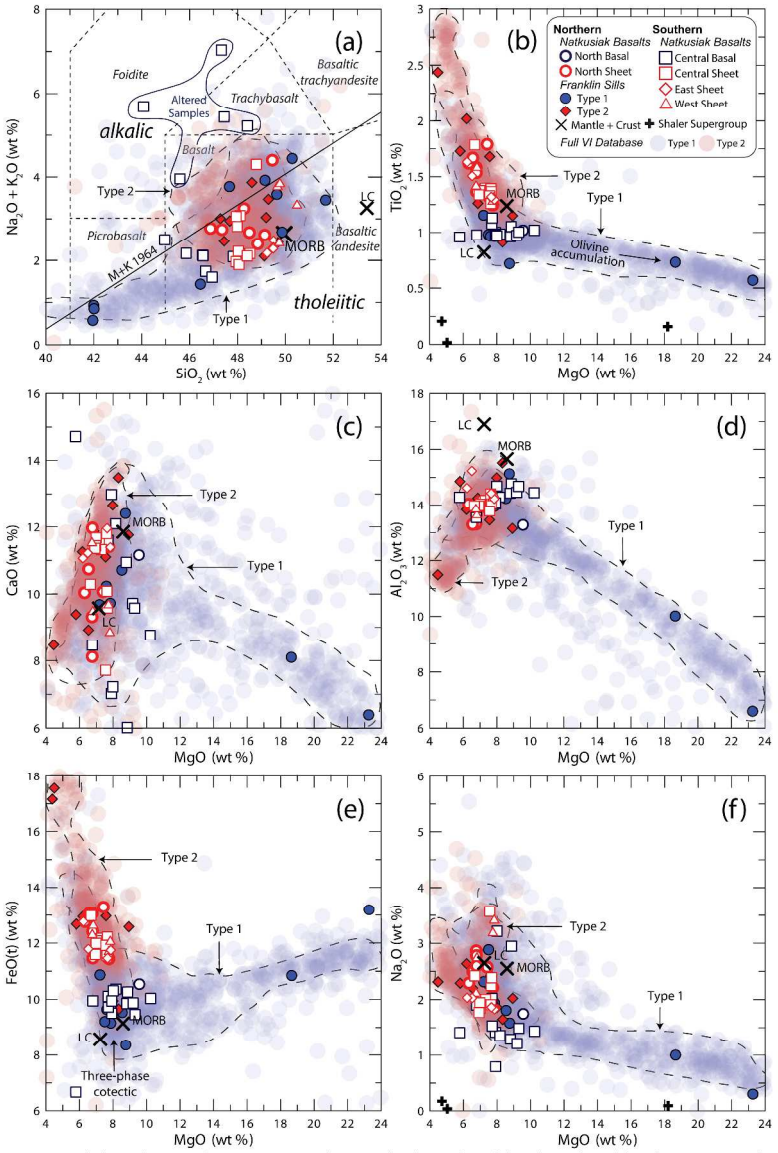

Figure 5. Whole-rock major-element variation diagrams for the Natkusiak basalts and Franklin sills on Victoria Island

546x819mm (300 x 300 DPI)

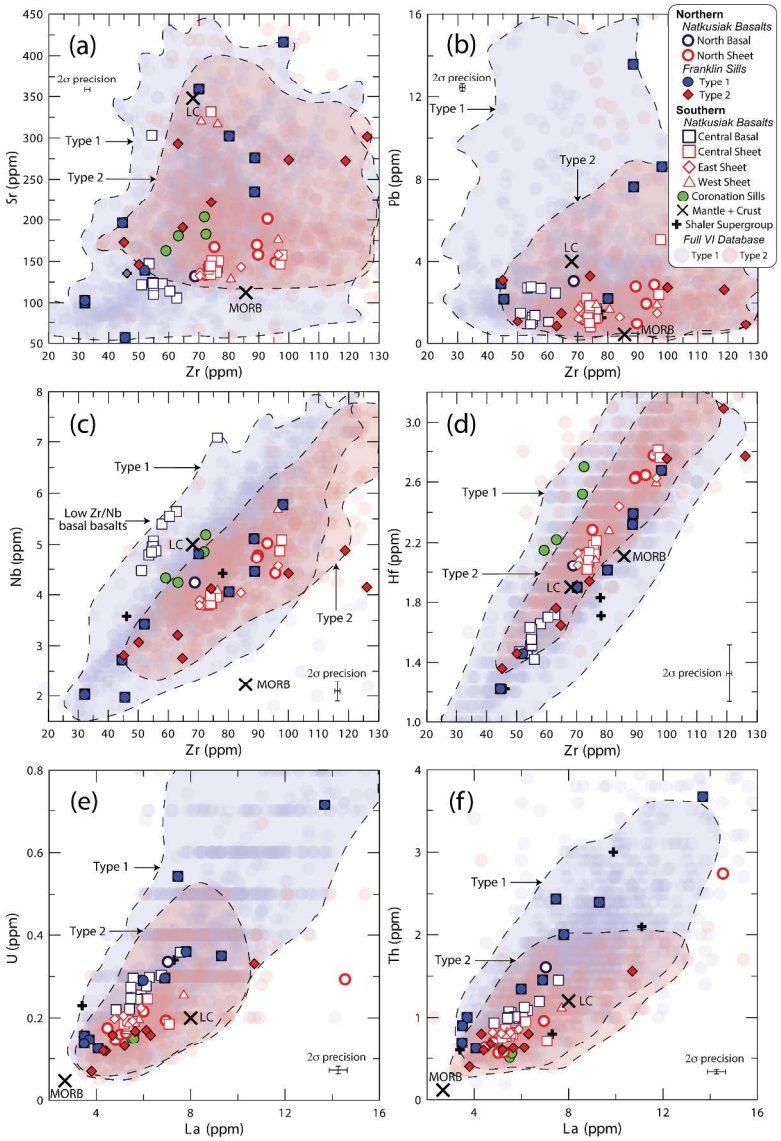

Figure 6. Whole-rock trace-element variation diagrams for the Natkusiak basalts and Franklin sills on Victoria Island

554x822mm (300 x 300 DPI)

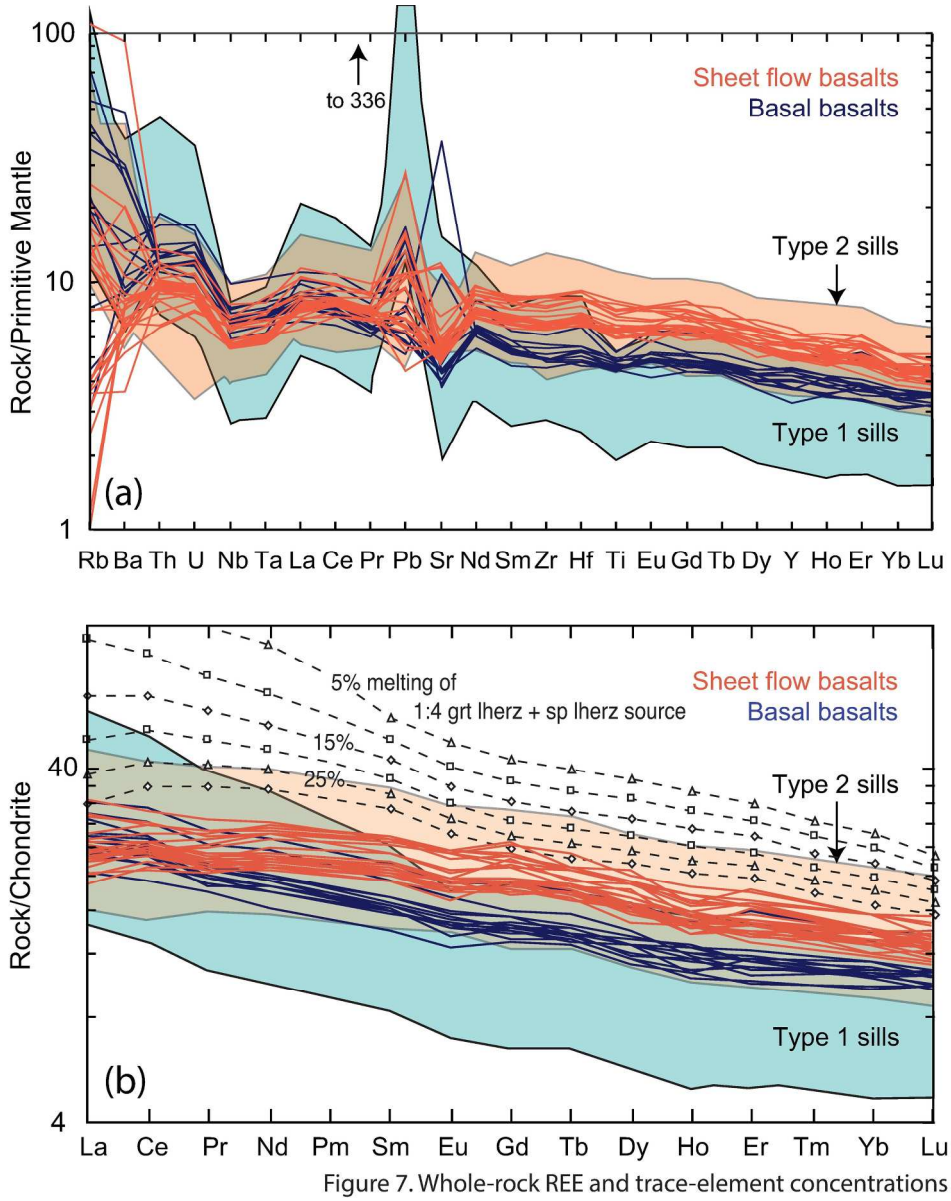

Figure 7. Whole-rock REE and trace-element concentrations

216x266mm (300 x 300 DPI)

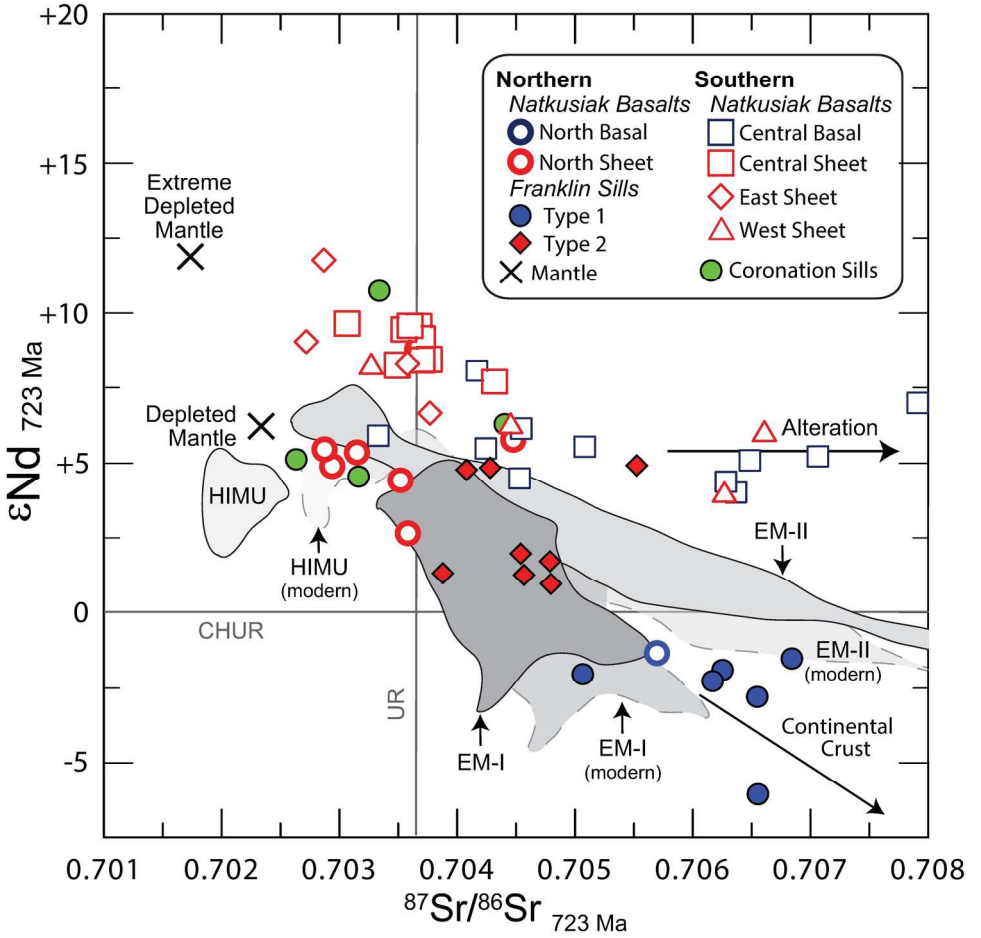

Figure 8. Whole-rock initial εNd and 87Sr/86Sr compositions

185x186mm (300 x 300 DPI)

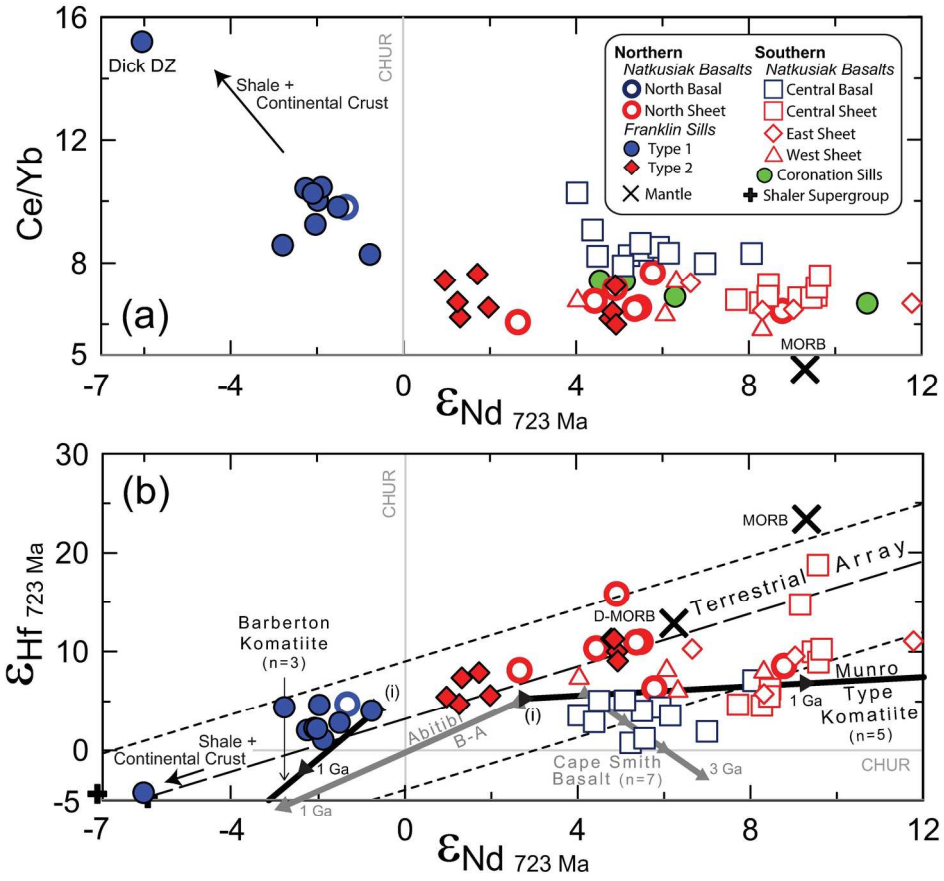

Figure 9. Whole-rock Ce/Yb, initial εNd and initial εHf diagrams

179x172mm (300 x 300 DPI)

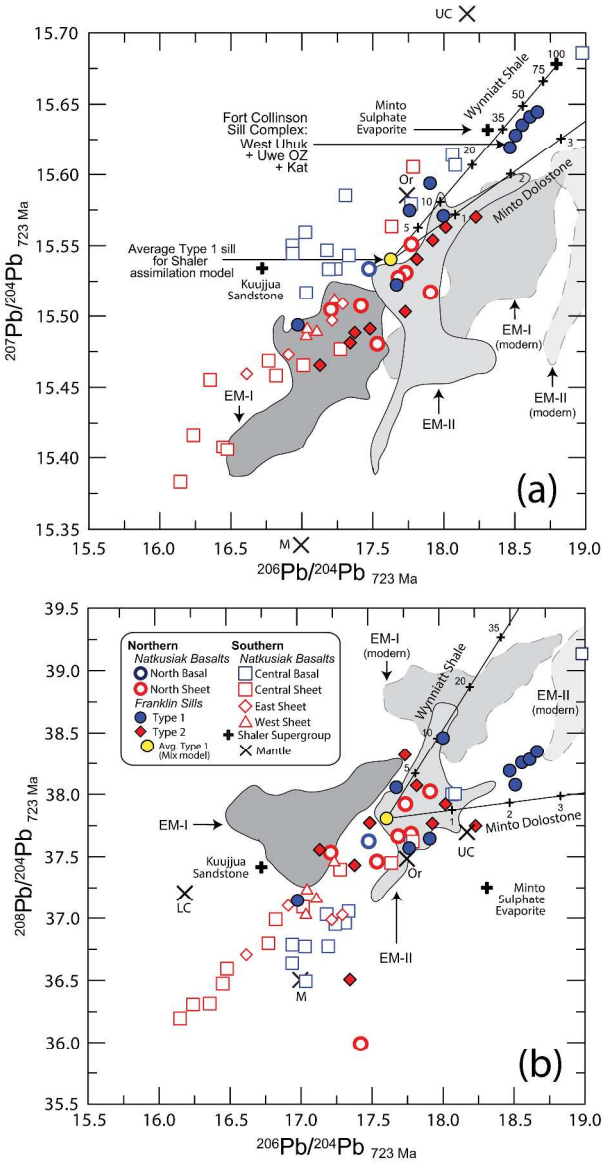

Figure 10. Whole-rock initial Pb isotope compositions, with Shaler assimilation model

368x691mm (300 x 300 DPI)

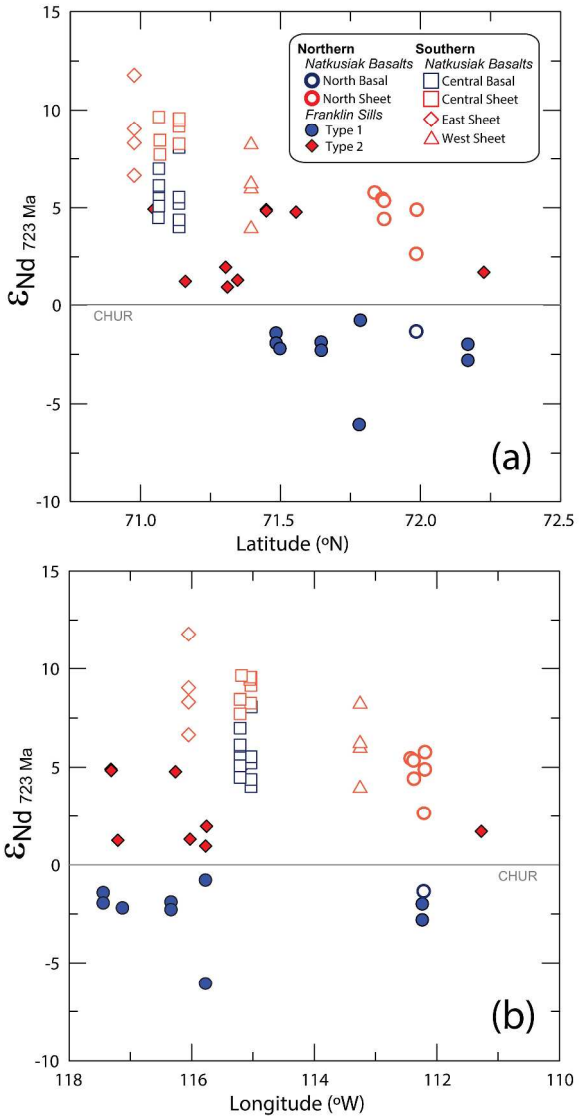

Figure 11. Spatial variations in whole-rock initial Nd isotope compositions

373x747mm (300 x 300 DPI)

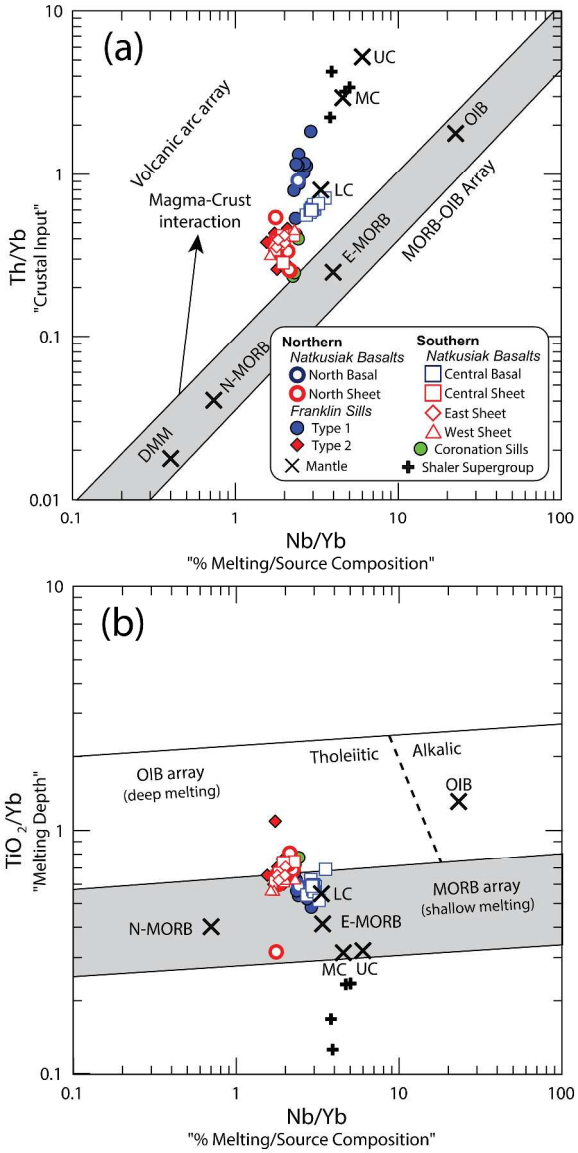

Figure 12. Th-Nb and Ti-Yb proxies for the Natkusiak basalts and Franklin sills on Victoria Island

374x783mm (300 x 300 DPI)

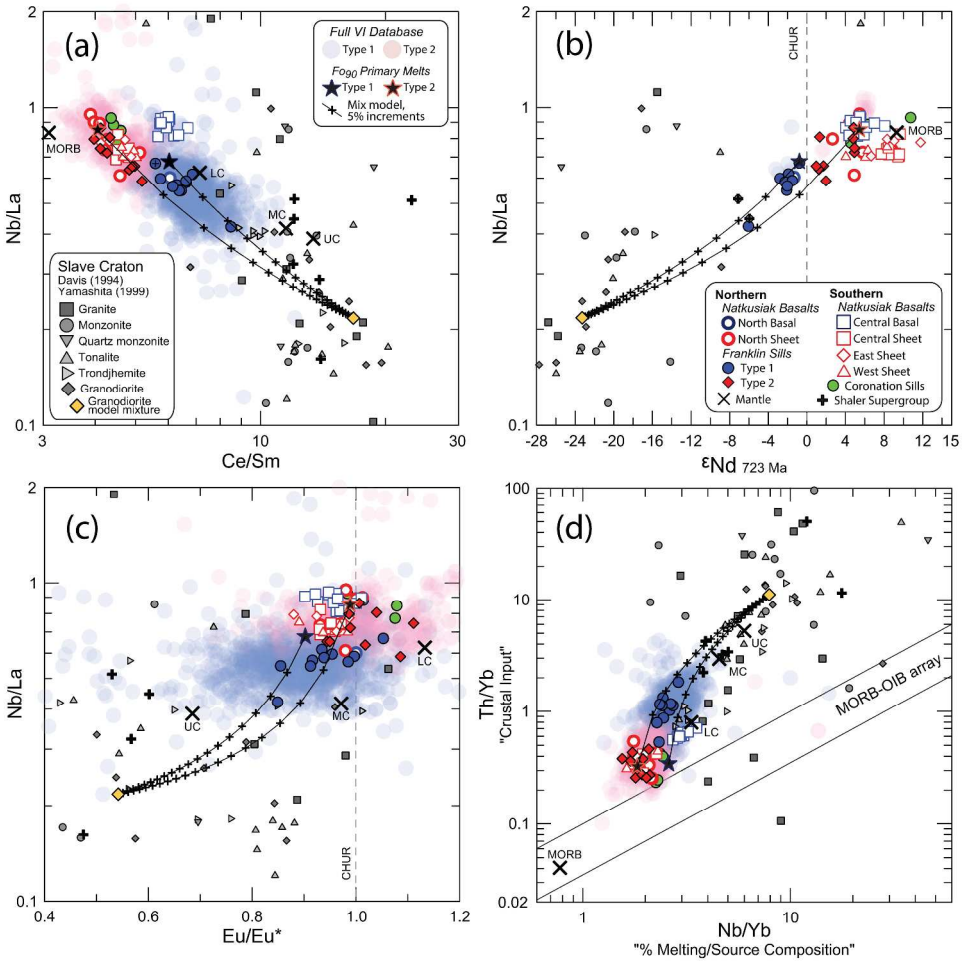

Figure 13. Whole-rock trace element and Nd-isotope diagrams showing mixtures between model primary melts and Slave province granitoids

382x398mm (300 x 300 DPI)

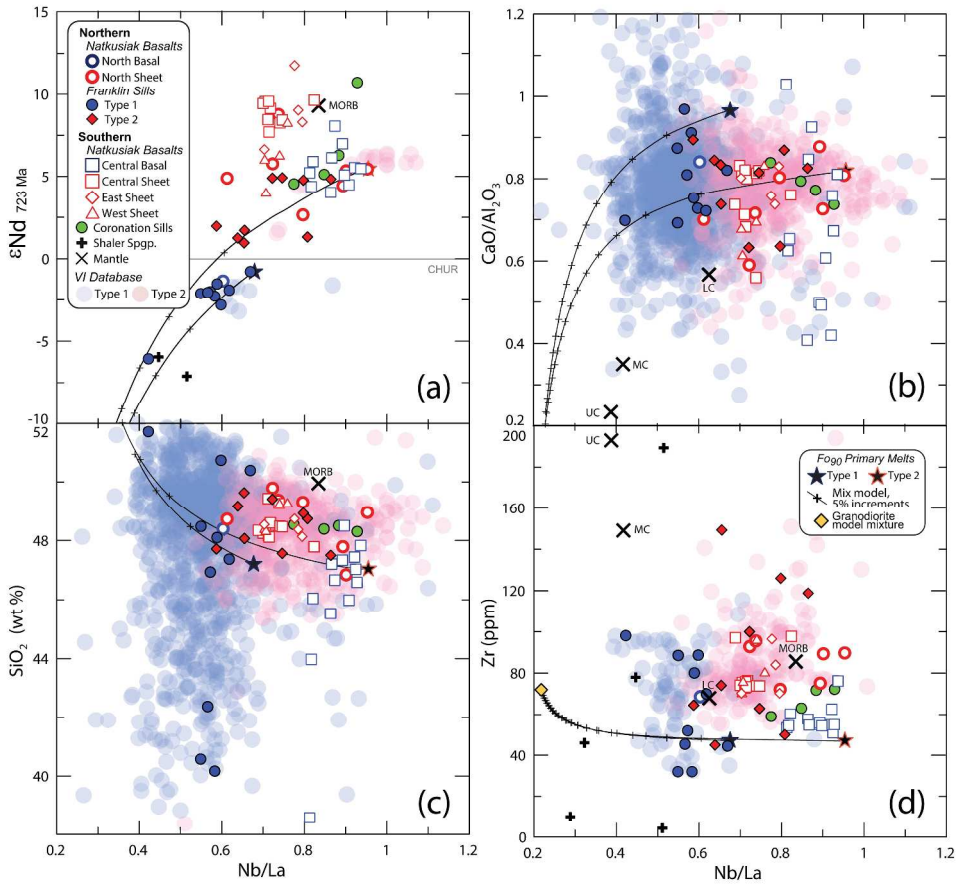

Figure 14. Variation of Nb/La with respect to εNd, CaO/Al_2O_3, SiO_2, and Zr

348x327mm (300 x 300 DPI)

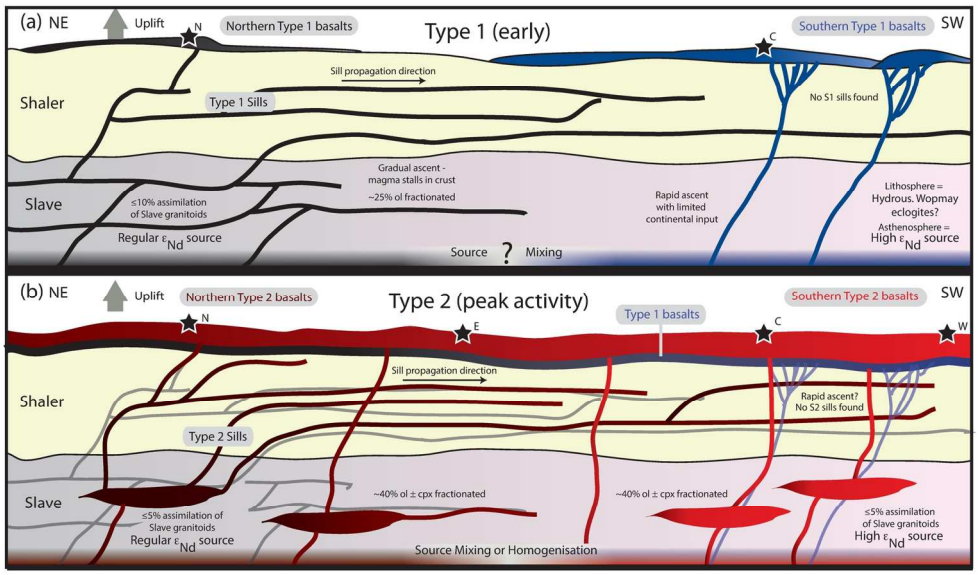

Figure 15. Schematic cross sections showing the development of the Franklin LIP

156x98mm (300 x 300 DPI)

Table 1: Whole rock $^{143}Nd/^{144}Nd$ and $^{176}Hf/^{177}Hf$ isotopic compositions of Natkusiak basalts and Franklin sills

Sample	Group	Unit	$^{143}Nd/^{144}Nd_m$	$2\sigma_m$	$^{147}Sm/^{144}Nd$	$^{143}Nd/^{144}Nd_i$	$\varepsilon_{Nd}(i)$	$^{176}Hf/^{177}Hf_m$	$2\sigma_m$	$^{176}Lu/^{177}Hf$	$^{176}Hf/^{177}Hf_i$	$\varepsilon_{Hf}(i)$
08JB04c1	N Type 1	V0 N	0.512401	6	0.1611	0.51164	-1.3	0.282695	5	0.0182	0.28244	4.7
08JB-06	N Type 2	V1 N	0.512731	7	0.1877	0.51184	2.7	0.282835	4	0.0214	0.28254	8.1
08JB07	N Type 2	V1 N	0.512816	9	0.1811	0.51196	4.9	0.282867	4	0.0082	0.28275	15.8
BL136	N Type 2	V1 N	0.512810	7	0.1706	0.51200	5.8	0.282752	5	0.0184	0.28249	6.7
BL144	N Type 2	V1 N	0.513017	7	0.1817	0.51216	8.8	0.282830	24	0.0193	0.28256	9.0
08JB01	N Type 2	V2 N	0.512878	8	0.1883	0.51199	5.5	0.282869	5	0.0180	0.28262	11.0
08JB01 (dup)			0.512882	7	0.1883	0.51199	5.5	0.282869	4	0.0180	0.28262	11.0
08JB02	N Type 2	V2 N	0.512881	10	0.1900	0.51198	5.4	0.282853	5	0.0170	0.28261	10.9
08JB04b	N Type 2	V2 N	0.512828	8	0.1888	0.51193	4.4	0.282838	5	0.0172	0.28260	10.3
TD15A2	S Type 1	V0 C	0.512941	8	0.1713	0.51213	8.3	0.282840	8	0.0238	0.28251	7.1
TD16A1	S Type 1	V0 C	0.512823	9	0.1739	0.51200	5.7	0.282672	6	0.0246	0.28233	0.8
TD18A2	S Type 1	V0 C	0.512689	8	0.1596	0.51193	4.4	0.282692	7	0.0203	0.28241	3.6
TD18A1	S Type 1	V0 C	0.512732	7	0.1666	0.51194	4.6	0.282696	5	0.0220	0.28239	2.9
TD16A3	S Type 1	V0 C	0.512805	5	0.1706	0.51200	5.7	0.282648	6	0.0219	0.28234	1.2
TD57A1	S Type 1	V0 C	-	-	-	-	-	0.282794	13	0.0229	0.28247	5.9
TD56A1*	S Type 1	V0 C	0.512740	9	0.1695	0.51194	4.5	0.282763	36	0.0225	0.28245	5.0
TD55A1	S Type 1	V0 C	-	-	-	-	-	0.282760	17	0.0225	0.28244	4.9
TD55A7*	S Type 1	V0 C	0.512788	6	0.1641	0.51201	5.9	0.282729	9	0.0213	0.28243	4.4
TD55A3*	S Type 1	V0 C	0.512810	6	0.1664	0.51202	6.2	0.282717	12	0.0221	0.28241	3.6
TD55A4*	S Type 1	V0 C	0.512779	7	0.1670	0.51199	5.5	0.282737	7	0.0226	0.28242	4.0
TD55A5	S Type 1	V0 C	0.512888	7	0.1717	0.51207	7.2	0.282732	7	0.0265	0.28236	1.9
TD55A6	S Type 1	V0 C	0.512779	6	0.1698	0.51197	5.2	0.282760	6	0.0221	0.28245	5.1
TD55A6 (dup)*			0.512451	8	0.1698	0.51165	-1.2	0.282769	5	0.0221	0.28246	5.4
TD17B1	S2	V1 C	0.513082	6	0.1847	0.51221	9.8	0.283109	5	0.0195	0.28284	18.8

Whole rock Nd and Hf isotopic compositions of Natkusiak basalts and Franklin sills with age corrections to 723 Ma. 'm' indicates measured isotopic ratios, 'i' are initial isotopic ratios at 723 Ma. $2\sigma_m$ is the absolute uncertainty on isotope ratio measurements at the two standard deviation confidence level. (dup) indicates a complete chemistry duplicate. Nd isotope ratios for samples marked '*' were measured by thermal ionization mass spectrometry; all other Nd isotope compositions were determined by MC-ICP-MS. All isotopic analyses were performed at the PCIGR. The laboratories at which trace elements were measured are indicated in the Supplementary data electronic appendices. *Groups*: N1, Northern Type 1 magmas; N2, Northern Type 2 magmas; S1, Southern Type 1 magmas;

S2, Southern Type 2 magmas. *Volcanic sections*: V0, basal basalts; V1, Sheet flow cycle 1; V2, Sheet flow cycle 2. N, Northern section, C, Central Section; E, Eastern Section; W, Western Section. *Sills*: OZ is the olivine-rich base of layered Type 1 sills, DZ is overlying diabasic roof zone.

Table 1: continued

Sample	Group	Unit	$^{143}Nd/^{144}Nd_m$	$2\sigma_m$	$^{147}Sm/^{144}Nd$	$^{143}Nd/^{144}Nd_i$	$\varepsilon_{Nd}(i)$	$^{176}Hf/^{177}Hf_m$	$2\sigma_m$	$^{176}Lu/^{177}Hf$	$^{176}Hf/^{177}Hf_i$	$\varepsilon_{Hf}(i)$
TD17B2	S2	V1 C	0.513066	8	0.1837	0.51220	9.6	0.283009	6	0.0204	0.28272	14.8
TD19A1	S2	V1 C	0.513084	7	0.1861	0.51220	9.7	0.282882	8	0.0209	0.28259	10.0
TD19A1 (dup)*			0.513094	8	0.1861	0.51221	9.9	0.282785	6	0.0209	0.28249	6.6
TD20A1	S2	V1 C	0.513086	8	0.1860	0.51220	9.7	0.282848	9	0.0207	0.28256	8.9
TD21A1	S2	V1 C	0.513004	7	0.1819	0.51214	8.5	0.282725	18	0.0207	0.28243	4.6
TD61A1	S2	V1 C	-	-	-	-	-	0.282841	17	0.0178	0.28259	10.1
TD61A2*	S2	V1 C	0.513076	6	0.1847	0.51220	9.7	0.282835	18	0.0171	0.28259	10.2
TD60B1*	S2	V1 C	0.513004	10	0.1822	0.51214	8.5	0.282782	7	0.0214	0.28248	6.2
TD60B3*	S2	V1 C	0.512968	7	0.1826	0.51210	7.7	0.282726	10	0.0206	0.28244	4.6
TD60B4	S2	V1 C	-	-	-	-	-	0.282786	6	0.0215	0.28248	6.3
TD60B5*	S2	V1 C	0.513037	8	0.1824	0.51217	9.1	0.282734	7	0.0195	0.28246	5.5
TD72B	S2	V1 E	0.512862	6	0.1785	0.51202	6.1	0.282848	23	0.0212	0.28255	8.7
TD72C	S2	V1 E	0.512767	8	0.1803	0.51191	4.0	0.282826	6	0.0210	0.28253	8.0
TD72D	S2	V1 E	0.512859	7	0.1750	0.51203	6.3	0.282773	24	0.0196	0.28250	6.8
TD72G	S2	V1 E	0.513021	7	0.1878	0.51213	8.3	0.282839	4	0.0205	0.28255	8.7
TD129A	S2	V1 W	0.513051	7	0.1862	0.51217	9.0	0.282840	7	0.0176	0.28259	10.2
TD129B	S2	V1 W	0.513189	8	0.1858	0.51231	11.8	0.282874	25	0.0176	0.28263	11.4
TD129E	S2	V1 W	0.512924	9	0.1851	0.51205	6.7	0.282872	25	0.0188	0.28261	10.7
TD129G	S2	V1 W	0.512989	7	0.1810	0.51213	8.3	0.282782	6	0.0213	0.28248	6.3
08JB311	N1	Dick DZ	0.512055	8	0.1390	0.51140	-6.1	0.282410	6	0.0160	0.28218	-4.3
08JB318	N1	Dick OZ	0.512469	7	0.1694	0.51167	-0.8	0.282703	7	0.0202	0.28242	4.0
08JB115	N1	Uwe DZ	0.512372	8	0.1707	0.51156	-2.8	0.282647	7	0.0155	0.28243	4.4
08JB166a	N1	Uwe OZ	0.512365	5	0.1603	0.51160	-2.0	0.282662	6	0.0161	0.28244	4.6
08JB166a (dup)			-	-	-	-	-	0.282661	5	0.0161	0.28244	4.6

Table 1: continued

Sample	Group	Unit	$^{143}Nd/^{144}Nd_m$	$2\sigma_m$	$^{147}Sm/^{144}Nd$	$^{143}Nd/^{144}Nd_i$	$\varepsilon_{Nd}(i)$	$^{176}Hf/^{177}Hf_m$	$2\sigma_m$	$^{176}Lu/^{177}Hf$	$^{176}Hf/^{177}Hf_i$	$\varepsilon_{Hf}(i)$
KS95A15	N1	WUS DZ	0.512346	12	0.1554	0.51161	-1.9	0.282620	6	0.0202	0.28234	1.1
KS95A6	N1	WUS OZ	0.512352	8	0.1608	0.51159	-2.3	0.282659	9	0.0211	0.28236	2.0
KS75A6	N1	Kat DZ	-	-	-	-	-	0.282657	5	0.0196	0.28238	2.7
KS74A8	N1	Kat OZ	0.512371	20	0.1628	0.51160	-2.1	0.282658	9	0.0206	0.28237	2.2
BH167A8	N1	LPS DZ	0.512359	7	0.1540	0.51163	-1.5	0.282645	5	0.0185	0.28238	2.8
BH167A2	N1	LPS OZ	0.512357	7	0.1593	0.51160	-2.0	0.282666	8	0.0213	0.28237	2.2
08JB12	N2	Type 2	0.512613	8	0.1728	0.51179	1.7	0.282788	5	0.0185	0.28253	7.9
08JB12 (dup)			-	-	-	-	-	0.282791	5	0.0185	0.28253	8.0
NW2A1	N2	Type 2	0.512617	6	0.1781	0.51177	1.3	0.282801	6	0.0204	0.28251	7.4
NW2A1 (dup)			-	-	-	-	-	0.282790	4	0.0204	0.28250	7.0
BH116A	N2	Type 2	0.512626	5	0.1806	0.51177	1.3	0.282805	6	0.0261	0.28244	4.7
JB123A	N2	Type 2	0.512604	6	0.1791	0.51176	1.0	0.282788	5	0.0234	0.28246	5.4
JB123A (dup)			0.512599	6	0.1791	0.51175	0.9	0.282784	6	0.0234	0.28245	5.3
MH129A2	N2	Type 2	0.512615	6	0.1704	0.51181	2.0	0.282812	5	0.0249	0.28246	5.6
MH129A2 (dup)			-	-	-	-	-	0.282794	4	0.0249	0.28244	4.9
HY74B2	N2	Type 2	0.512864	6	0.1926	0.51195	4.8	0.282876	4	0.0180	0.28262	11.3
08JB504	N2	Type 2	0.512815	6	0.1809	0.51196	4.9	0.282832	6	0.0173	0.28259	10.0
K5083A7	N2	Type 2	0.512861	6	0.1914	0.51195	4.8	0.282854	6	0.0164	0.28262	11.3
BH362A	N2	Type 2	0.512857	6	0.1896	0.51196	4.9	0.282879	5	0.0226	0.28256	9.1
BH362A (dup)			0.512859	6	0.1896	0.51196	5.0	0.282876	4	0.0226	0.28256	9.0
MH170A1	Shaler	KuujSst	0.511980	7	0.1121	0.51145	-5.0	-	-	-	-	-
HY69A1	Shaler	WnShl	0.511908	7	0.1194	0.51134	-7.1	0.282379	5	0.0141	0.28218	-4.4
HY74A2b	Shaler	MntDol	-	-	-	-	-	0.282395	37	0.0160	0.28217	-4.8
HY64A1	Shaler	BtLst	0.511967	6	0.1194	0.51140	-6.0	0.282335	9	0.0118	0.28217	-4.8

Table 2: Whole rock $^{86}Sr/^{87}Sr$ and radiogenic Pb isotopic compositions of Natkusiak basalts and Franklin sills

Sample	Group	Unit	$^{87}Sr/^{86}Sr_m$	$2\sigma_m$	$^{87}Rb/^{86}Sr$	$^{87}Sr/^{86}Sr_i$	$^{208}Pb/^{204}Pb_m$	$2\sigma_m$	$^{207}Pb/^{204}Pb_m$	$2\sigma_m$	$^{206}Pb/^{204}Pb_m$	$2\sigma_m$	$^{208}Pb/^{204}Pb_i$	$^{207}Pb/^{204}Pb_i$	$^{206}Pb/^{204}Pb_i$
08JB04c1	N Type 1	V0 N	0.706130	8	0.0423	0.70569	38.8839	28	15.5865	11	18.3063	12	37.625	15.534	17.476
08JB-06	N Type 2	V1 N	0.704010	8	0.0418	0.70358	38.9902	35	15.5649	13	18.1590	12	37.534	15.505	17.208
08JB07	N Type 2	V1 N	0.704733	8	0.1742	0.70294	38.9412	34	15.5705	12	18.4153	14	35.992	15.507	17.420
BL136	N Type 2	V1 N	0.714454	9	0.9672	0.70447	39.0957	16	15.5786	6	18.4842	7	37.923	15.531	17.735
BL144	N Type 2	V1 N	0.704154	9	0.0482	0.70366	38.5073	17	15.5868	6	18.3384	6	37.685	15.551	17.775
08JB01	N Type 2	V2 N	0.703306	9	0.0423	0.70287	38.8471	27	15.5589	12	18.7726	18	37.463	15.480	17.535
08JB01 (dup)			0.703304	8	0.0423	0.70287	38.8479	33	15.5590	8	18.7737	8	37.464	15.480	17.536
08JB02	N Type 2	V2 N	0.703592	9	0.0432	0.70315	38.5140	35	15.5452	11	18.3504	12	38.025	15.517	17.909
08JB04b	N Type 2	V2 N	0.703874	9	0.0349	0.70351	38.8334	28	15.5913	11	18.6897	13	37.666	15.528	17.684
TD15A2	S Type 1	V0 C	0.705379	8	0.1177	0.70416	38.9555	146	15.6669	58	18.7763	64	36.639	15.550	16.937
TD16A1	S Type 1	V0 C	0.712673	8	0.5440	0.70706	40.0372	30	15.7324	11	19.7116	13	39.136	15.686	18.979
TD18A2	S Type 1	V0 C	0.709335	8	0.2878	0.70636	38.9728	10	15.6674	4	18.9047	4	38.000	15.614	18.064
TD18A1	S Type 1	V0 C	0.712353	8	0.5885	0.70628	38.8769	19	15.6497	7	18.7613	8	38.005	15.607	18.084
TD16A3	S Type 1	V0 C	0.711209	8	0.5939	0.70508	38.6970	12	15.6330	5	18.6213	6	37.608	15.579	17.773
TD57A1	S Type 1	V0 C	0.707342	10	0.3213	0.70403	38.4430	72	15.6552	32	18.4109	32	36.963	15.585	17.310
TD56A1	S Type 1	V0 C	0.707659	8	0.3037	0.70453	38.9796	80	15.6827	31	18.9696	34	36.773	15.559	17.028
TD55A1	S Type 1	V0 C	0.706832	9	0.2997	0.70374	38.7384	71	15.6449	28	18.5185	33	36.788	15.545	16.939
TD55A7	S Type 1	V0 C	0.706992	7	0.3553	0.70333	39.7843	13	15.6865	4	19.3823	6	37.032	15.547	17.180
TD55A3	S Type 1	V0 C	0.705220	9	0.0658	0.70454	38.5582	24	15.6170	9	18.6131	8	36.494	15.517	17.034
TD55A4	S Type 1	V0 C	0.706079	9	0.1782	0.70424	38.9888	11	15.6346	4	18.8300	4	36.953	15.534	17.242
TD55A5	S Type 1	V0 C	0.709210	8	0.1262	0.70791	38.7736	10	15.6281	4	18.6724	4	37.057	15.543	17.335
TD55A6	S Type 1	V0 C	0.709855	8	0.3268	0.70648	39.3151	25	15.6471	10	18.9822	14	36.775	15.534	17.192
TD55A6 (dup)			0.709790	9	0.3268	0.70642	39.2646	8	15.6479	7	18.9722	20	36.726	15.534	17.184
TD17B1	S2	V1 C	0.703801	8	0.0125	0.70367	37.7371	43	15.4580	16	17.3270	17	36.197	15.383	16.147

Whole rock Sr and Pb isotopic compositions of Natkusiak basalts and Franklin sills with age corrections to 723 Ma. Group and unit labels as described for Table 1. 'm' indicates measured isotopic ratios, 'i' are initial isotopic ratios at 723 Ma. $2\sigma_m$ is the absolute uncertainty on isotope ratio measurements at the two standard deviation confidence level. (dup) indicates a complete chemistry duplicate. All isotopic analyses were performed at the PCIGR. The laboratories at which trace elements were measured are indicated in the Supplementary data electronic appendices.

Table 2: continued

Sample	Group	Unit	$^{87}Sr/^{86}Sr_m$	$2\sigma_m$	$^{87}Rb/^{86}Sr$	$^{87}Sr/^{86}Sr_i$	$^{208}Pb/^{204}Pb_m$	$2\sigma_m$	$^{207}Pb/^{204}Pb_m$	$2\sigma_m$	$^{206}Pb/^{204}Pb_m$	$2\sigma_m$	$^{208}Pb/^{204}Pb_i$	$^{207}Pb/^{204}Pb_i$	$^{206}Pb/^{204}Pb_i$
TD17B2	S2	V1 C	0.703846	8	0.0141	0.70370	37.8842	66	15.4904	25	17.4061	29	36.309	15.416	16.239
TD19A1	S2	V1 C	0.703846	8	0.0293	0.70354	38.7817	16	15.5194	10	18.2078	7	36.476	15.408	16.448
TD19A1 (dup)			0.703838	7	0.0293	0.70354	38.8047	20	15.5208	7	18.2260	8	36.498	15.409	16.466
TD20A1	S2	V1 C	0.704644	8	0.1015	0.70360	38.1422	17	15.4794	7	17.6362	7	36.595	15.406	16.478
TD21A1	S2	V1 C	0.703984	9	0.0480	0.70349	38.3143	48	15.5237	19	17.8522	22	36.991	15.458	16.822
TD61A1	S2	V1 C	0.704164	8	0.1603	0.70251	38.1509	78	15.6000	33	18.2119	36	37.451	15.563	17.636
TD61A2	S2	V1 C	0.703503	7	0.0428	0.70306	38.0677	62	15.6285	26	18.1516	29	37.623	15.605	17.788
TD60B1	S2	V1 C	0.706265	8	0.2429	0.70376	38.2121	11	15.5135	4	17.8547	5	37.397	15.477	17.275
TD60B3	S2	V1 C	0.706148	7	0.1778	0.70431	38.2154	69	15.5347	27	17.8116	31	36.799	15.469	16.770
TD60B4	S2	V1 C	0.707441	7	0.1347	0.70605	38.0427	10	15.5122	4	17.7502	4	37.092	15.466	17.014
TD60B5	S2	V1 C	0.704233	9	0.0518	0.70370	38.3121	61	15.5458	25	17.7850	26	36.316	15.455	16.357
TD72B	S2	V1 E	0.707562	9	0.0926	0.70661	38.1941	38	15.5366	15	17.8432	16	37.170	15.490	17.109
TD72C	S2	V1 E	0.707013	8	0.0724	0.70627	38.0573	15	15.5343	6	17.7807	6	37.039	15.487	17.034
TD72D	S2	V1 E	0.706620	9	0.2102	0.70445	38.6005	18	15.5540	6	18.0206	7	37.244	15.492	17.042
TD72G	S2	V1 E	0.704921	9	0.1603	0.70327	38.5575	16	15.5642	6	18.0438	6	37.469	15.513	17.233
TD129A	S2	V1 W	0.704806	10	0.2027	0.70271	38.4971	28	15.5836	11	18.4704	12	37.027	15.509	17.291
TD129B	S2	V1 W	0.704263	9	0.1355	0.70286	38.3390	34	15.5676	14	18.3296	16	36.987	15.497	17.216
TD129E	S2	V1 W	0.705482	9	0.1663	0.70377	38.2250	31	15.5260	10	17.7444	12	37.103	15.473	16.910
TD129G	S2	V1 W	0.704658	8	0.1050	0.70357	38.2808	17	15.5352	9	17.8089	9	36.707	15.459	16.615
08JB311	N1	Dick DZ	0.709325	8	0.2688	0.70655	38.6694	21	15.6338	9	18.5345	9	37.646	15.594	17.906
08JB318	N1	Dick OZ	-	-	-	-	38.5644	18	15.5430	7	17.9936	7	38.057	15.523	17.671
08JB115	N1	Uwe DZ	0.710803	7	0.4126	0.70654	38.3304	16	15.6086	6	18.2956	7	37.570	15.575	17.762
08JB166a	N1	Uwe OZ	-	-	-	-	38.3728	22	15.6403	9	18.6339	10	38.258	15.635	18.555
08JB166a (dup)			-	-	-	-	38.3951	18	15.6449	7	18.6504	8	38.280	15.640	18.572

Table 2: continued

Sample	Group	Unit	$^{87}Sr/^{86}Sr_m$	$2\sigma_m$	$^{87}Rb/^{86}Sr$	$^{87}Sr/^{86}Sr_i$	$^{208}Pb/^{204}Pb_m$	$2\sigma_m$	$^{207}Pb/^{204}Pb_m$	$2\sigma_m$	$^{206}Pb/^{204}Pb_m$	$2\sigma_m$	$^{208}Pb/^{204}Pb_i$	$^{207}Pb/^{204}Pb_i$	$^{206}Pb/^{204}Pb_i$
KS95A15	N1	WUS DZ	0.709112	8	0.2774	0.70625	38.4723	24	15.6479	13	18.7179	14	38.283	15.641	18.611
KS95A6	N1	WUS OZ	0.708347	8	0.2113	0.70617	38.3825	21	15.6457	8	18.6813	11	38.348	15.645	18.662
KS75A6	N1	Kat DZ	0.713665	8	0.5953	0.70752	38.5018	38	15.6403	14	18.7040	16	38.078	15.628	18.509
KS74A8	N1	Kat OZ	-	-	-	-	38.3183	23	15.6229	11	18.5280	8	38.191	15.619	18.469
BH167A8	N1	LPS DZ	0.713842	9	0.6786	0.70684	38.7096	24	15.5576	9	17.9820	10	37.146	15.494	16.975
BH167A2	N1	LPS OZ	0.710458	9	0.5227	0.70506	39.2212	24	15.6015	9	18.4815	11	38.460	15.571	18.000
08JB12	N2	Type 2	0.707290	10	0.2427	0.70479	38.1637	18	15.5194	7	17.8665	8	37.432	15.488	17.377
NW2A1	N2	Type 2	0.705406	8	0.1485	0.70387	38.6450	21	15.5216	7	17.9653	7	37.772	15.491	17.484
BH116A	N2	Type 2	0.705720	8	0.1121	0.70456	38.7815	22	15.5214	9	18.0205	9	38.320	15.503	17.732
JB123A	N2	Type 2	0.706429	8	0.1577	0.70480	38.6513	20	15.5634	8	18.1745	9	38.073	15.541	17.814
JB123A (dup)			0.706412	8	0.1577	0.70478	38.6442	18	15.5642	7	18.1668	7	38.066	15.541	17.806
MH129A2	N2	Type 2	0.706313	8	0.1722	0.70454	38.6285	18	15.5157	7	17.9225	7	37.557	15.466	17.131
MH129A2 (dup)			-	-	-	-	38.7646	19	15.5196	7	18.0039	9	37.693	15.469	17.212
HY74B2	N2	Type 2	0.708641	8	0.4424	0.70408	39.3284	23	15.6397	8	19.3250	9	37.749	15.570	18.229
08JB504	N2	Type 2	-	-	-	-	38.4714	22	15.5928	9	18.4857	10	37.923	15.563	18.017
K5083A7	N2	Type 2	0.707418	8	0.3044	0.70428	38.3321	25	15.5842	8	18.4033	8	37.767	15.554	17.925
BH362A	N2	Type 2	0.706174	8	0.0632	0.70552	38.7930	14	15.5498	5	18.4251	6	36.508	15.481	17.344
MH170A1	Shaler	KuujSst	-	-	-	-	38.6046	13	15.6353	5	18.3133	6	37.416	15.534	16.720
HY69A1	Shaler	WnShl	0.937212	10	19.6984	0.73394	42.9249	31	15.8096	11	20.8654	13	39.976	15.678	18.793
HY74A1a	Shaler	MntEvp	-	-	-	-	37.7587	23	15.6359	9	18.3727	9	37.252	15.632	18.309
HY74A2b	Shaler	MntDol	-	-	-	-	38.9264	22	16.0438	8	24.8360	12	38.737	15.984	23.897
BH166A1	Shaler	KilEvp	0.707150	8	0.0011	0.70714	39.7664	33	15.8334	13	21.9086	17	39.211	15.829	21.833
BH166A1 (dup)			0.707150	8	0.0011	0.70714	-	-	-	-	-	-	-	-	-
BH196A1	Shaler	WynCb	0.707724	8	0.0356	0.70736	41.7335	31	16.0771	12	25.4641	16	39.124	15.877	22.309
HY64A1	Shaler	BtLst	-	-	-	-	49.4652	29	17.6601	10	50.3386	26	40.517	15.846	21.741

Table 3: The four geochemical groups defined in the Franklin sills and Natkusiak basalts.

Magma type	Included units	Age	Interpretation
Northern Type 1 (Low Ti)	Type 1 sills and northern section basal basalts	Old	Mafic, continentally influenced, containing up to 10% granodiorite
Southern Type 1 (Low Ti)	Central section basal basalts	Old	Little continental influence. High eNd asthenospheric source
Northern Type 2 (High Ti)	Type 2 sills and northern section sheet flow basalts	Young	Fractionated, waning continental influence of up to 5% granodiorite
Southern Type 2 (High Ti)	Western, central and eastern section sheet flow basalts	Young	Fractionated, waning continental influence, High eNd source